

4

Anthropogenic Effects on Surface Water Quality Assessment in Baitarani River Basin, Odisha Using GIS and MCDM Techniques

Abhijeet Das

Department of Civil Engineering, C.V. Raman Global University, Bhubaneswar, India.

Email: das.abhijeetlaltu1999@gmail.com, abhijeetlaltu1994@gmail.com

Abstract

Surface water is necessary for the sustainable expansion of society, economy, and agriculture in and around Baitarani Basin, Odisha. 22 significant surface water regulating variables were collected from 13 locations during the 5-year (2018-2023) monsoon period and were, developed by combining entropy-based water quality index (EWQI) data and TOPSIS analysis was carried out to determine surface water prospect zones. The selected catchments and its spatial maps were designated and the anticipated surface water zone model's results were divided into four groups: excellent (15.38%), good (38.46%), medium (15.3%) and poor (30.77%). However, TOPSIS, a multi-objective judgement tool, was used to rank the sites based on their relative emissions of harmful pollutants. Findings suggest that St-8 obtained the highest performance score and was recognized, as perhaps, the most polluted location in comparison to other remaining sites. Urbanization, irrigation, landfills, and e-waste are the primary agents for water quality deterioration. Chemical indices such as SAR, RSC, MH, KI, PS, PI, CR, CAI-1, and CAI-2, were evaluated and the results demonstrated that the river is good for irrigation. USSL diagrams categorized the water samples as C1-S1 and C2-S1, respectively, which promotes irrigation suitability. From the Piper and Durov diagram plots, two different types of water were identified as Na⁺-Cl⁻ and Ca (HCO₃)₂. On the other hand, Gibb's plot implies that most samples fall under the evaporation-precipitation dominance.

Keywords

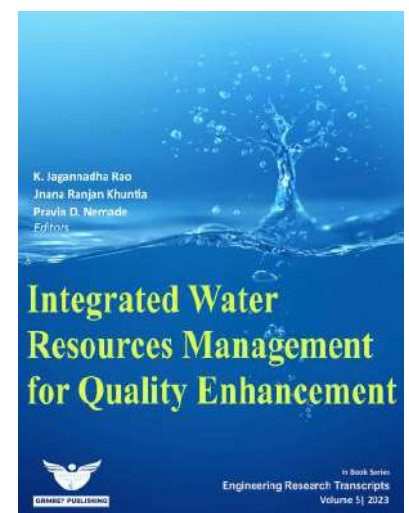
Baitarani Basin, EWQI, TOPSIS, USSL, Piper, Durov, Gibb's

Received: 25 Mar 2023 | Accepted: 20 Oct 2023 | Online: 30 Oct 2023

Cite this article

Abhijeet Das (2023). Anthropogenic Effects on Surface Water Quality Assessment in Baitarani River Basin, Odisha Using GIS and MCDM Techniques. *Engineering Research Transcripts*, 5, 37–64.

https://doi.org/10.55084/grinrey/ERT/978-81-964105-3-7_4



1. Introduction

Water, whether found above ground or beneath, is the most significant and vital natural resource for supporting life and for the sustainable growth of socioeconomic domains like irrigation and industry [1]. Throughout India, surface water is a naturally occurring, essential resource that is used for household and consumption needs [2]. Urbanization, climate change, and other Anthropogenic environmental disturbances have a significant adverse impact on surface water [3]. In recent years, this has caused a considerable decline in the quality of the water. Furthermore, extensive land use change, spontaneous urbanization, forest cover degradation/deforestation, high tourism pressures, landform degradation, uncontrolled fertilizer and pesticide use, and landform degradation have all had a significant impact on the biological and physiochemical characteristics of the river's water resources [4]. Stress on existing sources is higher now, as a consequence of, the unplanned inefficient management of surface water resources due to overexploitation for domestic, commercial, and industrial uses [5]. Therefore, changes in land use, cropping patterns, high water demand, high yielding crop races, and water availability are the factors that gets driven by surface water crisis.

However, insufficient management has spread the global water cycle even further, probably hastening climate change and surface water pollution [6]. Although safeguarding surface water is challenging and expensive, pollution often results from even prospective anthropogenic activity, which can go unnoticed for years [7]. The difficulties caused by eutrophication are primarily felt in developing nations, particularly those in the tropics, where constant sun input and hot temperatures support year-round algal blooms [8]. In a broader context, unplanned and unsustainable surface water use is having a severe impact on water storage [9]. It serves as complicated and is not suitable for human consumption or irrigation [10]. Water shortage has also become a global concern due to the regional effects of water quality degradation, abstraction, drought, floods, and irregular rainfall on a vast population [11]. The main problems in this area have appeared to be the irregular pattern of precipitation, soil loss due to erosion from unstable slopes, reservoir sedimentation, decreased soil productivity, and persistent crop failures [12]. However, pinpointing the areas where surface water may be present is essential for maintaining water quality and the surface water management system [13]. Consequently, the term "Water Quality Index (WQI)" is the best approach to describe whether a water body, like a river, is suitable for use, serving as a drinking water source for people [14]. It is often regarded to be based on wellbeing and consumption of people [15]. Over the past ten years, numerous research has utilized different WQIs [16, 17, 18, 19, 20]. Such investigations called for the expert judgment-based (Delphi technique) weighting of individual parameters in relation to the planned applications of the water, such as irrigation, drinking, and aquatic life [21].

The entropy-based method was chosen because it incorporates the intrinsic unpredictability of the variables and eliminates the subjectivity involved in weight allocation in traditional methodologies [22]. This approach is being well addressed by the past researchers as weighted entropy water quality index (EWQI). It defines as the result of adding the weights along with quality ratings of all the prerequisites to get a cumulative generated numerical rating/score [23]. It provides a cutting-edge workspace for spatiotemporal data that makes it possible to organize, visualize, and integrate digital geographic data from a variety of sources [20]. Through spatial analysis, modification, and visualization, Entropy and GIS work together to create a flexible and user-friendly solution that supports surface water management planning and decision-making [24]. Hence, these techniques have arisen to address the limitations of traditional WQIs, the modification of conflicts between various WQIs by entropy-based MCDMs, and the optimization of online monitoring systems to further the information gleaned from monitoring programs [25].

Furthermore, Multi-criteria decision-making (MCDM) study had to be added to the assessment of water quality in order to ascertain the complicated relationships between the quality parameters and testing sites. On the other hand, experts have applied the techniques to decision-making for many years to determine surface water potential zones by weighting thematic layers [26]. Since last few years, by employing MCDM,

to monitor water quality, it initiates to produce better results on account of its reduction in the subjectivity in criteria selection and vast application fields [27, 28, 29]. Another important technique in MCDM, addressed as 'The Technique for Order of Preference by Similarity to Ideal Solution (TOPSIS)'. This methodology is also considered to be an appropriate framework for outranking possibilities and fixing decision-making challenges [30]. This method also uses information entropy to find a scenario that is further away from the negative ideal solution (NIS) but closer to the positive ideal solution (PIS) (NIS). This approach is suggested when there are inadequate data for analysis, to split up several substitutions into pair-wise comparisons, and to combine the results [31]. In order to provide decision-makers with information on suitability assessments of agricultural systems, [28] coupled GIS with MCDM technique by creating weights of the various layers that were received from the GIS environment. GIS technology has been employed recently to continuously monitor surface water quality [5]. It is implemented as a data warehouse to construct images of water quality based on concentration values of different chemical components, and is regarded as mostly a powerful mechanism for mapping the water quality and effective for measurement [32]. Further, in the current study region, its output can serve as baseline data for other surface water-related studies. It is noticed that more precise estimates of the surface water quality zone are made using hydrological investigations and Geospatial modelling [33]. The geographic variability of point attributes is interpolated by the geospatial algorithms like Kriging and inverse distance weighted (IDW), which also predict for an unobserved location using adjacent known attributes [34]. Periodic data management using GIS and IDW interpolation has been made possible by the implications of spatial and temporal trends appraisal of pollution in the water resources [35].

Further, GIS is used to analyse and present spatial data, facilitating resource planning and environmental preservation [36]. Researchers have discovered that geo-statistical modelling is a cutting-edge method, that is crucial for giving a complete picture of surface water quality, which is crucial for effectively managing and safeguarding these important resources [37]. Hence, IDW is nowadays considered as an effective tool for spatial interpolation [38] and its nearest specified sites were taken into account while calculating weights for different variables at specific location focused on distance [39]. Additionally, employing normally distributed known data, this interpolation technique is the most effective and extensively used method for estimating unknown values i.e., attributes [40]. GIS and remote sensing are tools for adaptable and user-friendly surface water management and decision-making. Although [41] used the WQI and IDW process to examine the water quality of the Tigris River in Iraq for drinking purposes, the findings revealed roughly 38% of the wells there categorized as being poor water. Generally, rivers are crucial to the irrigation of this area for the growth of crops and feed [42]. It is seen that hydrological and socioeconomic variables, as well as time-sensitive undulation in the source and configuration of revived water, may cause irregular variations in the metrics relating to water quality. As a result, the GIS tool is capable, quick, and applicable for 3D planning due to its ability to manage complicated issues, huge data banks, and data retrieval [43]. However, due to conventional and inefficient livestock farming techniques, such as poor soil quality, scarce fodder supplies, limited water availability, and harsh climate, it influences the behaviour of water for its human consumption [44].

Likewise, the agricultural industry of the region should be greatly and substantially expanded with increased production-scale activities [45]. To be able to review the water quality for cultivation purpose, the major indices like magnesium hazard (MH), sodium percentage (% Na), corrosivity ratio (CR), permeability index (PS), Chloroalkaline indices 1 (CAI-1), sodium adsorption ratio (SAR), potential salinity (PS) residual sodium carbonate (RSC), Chloroalkaline indices 2 (CAI-2) and Kelly's ratio (KR) are required to be examined. To better comprehend the effects of contaminants, the spatial distribution of a few pollutants was also explored [46]. To give a straightforward and practical tool for judgement on the condition of surface water, a combined framework of EWQI, TOPSIS, GIS and irrigation indices in screening and maintenance of water quality can be proposed. This topic was carried out to evaluate the Baitarani River water quality in the State of Odisha, India. Until now, less thorough research studies on integrated methodology based on

EWQI, GIS, MCDM and agricultural parameters has been carried out across the river's catchment area in a contrast to identify primary pollution sources and how they affect surface river systems [47, 48]. There seems to be a study gap in this area, however further analysis is required to better understand the depth and sources of pollution. Furthermore, the utilization or utility of the EWQI, MCDM technique such as TOPSIS for the thorough water quality evaluation, which constitutes the innovative aspect of the present work. Also, the river was investigated depending upon the monthly data sources to determine whether it is suitable for irrigation for spatiotemporal variability taking RSC, CR, SAR, PI, KR, PS, CAI-1, MH, % Na, and CAI-2. Hence, the present work aimed to evaluate whether surface water is fit for consumption and agriculture, using the above discussed approaches. Therefore, the subsequent findings would offer a snapshot of the water quality, with reference to urban outflows and other anthropogenic factors. This study aids in choosing relevant locations for the construction of conservation infrastructure such as agricultural ponds, check dams, trenches, and water holding structures.

2. Description of the Study Area

The river Baitarani plays a vital role in the Peninsular River system in India. It is often regarded as one of the six major rivers of Odisha, and it is located between 32 and 1024 meters above the sea level. Currently, this river is a key element that makes it a top tourist destination and is largely comprised of aquatic animals, wildlife, and vegetation. It begins to emerge from the Gupta Ganga mountains in the Keonjhar district of Odisha at an altitude of 900 m. The geographical coordinates fall within the basin consisting of $21^{\circ}31'N$ latitude and $85^{\circ}33'E$ longitude (Figure 1).



Fig. 1. Map of Study Area

Consequently, this river extends over a length of 360 km from Gonasika to the Bay of Bengal. The basin is largely covered with agricultural land, with the area comprising of 14351 km² in Odisha [49]. The basin's average annual rainfall stretches between 1400 to 1600 mm, covering nearly 90% of the basin. Multi-residential structures, reasonable housing, accommodation, temples, and educational institutions, shopping malls, laundromats, parking lots, and various paved and unpaved roads are among the residential and commercial developments that are still being built in this basin [50]. For instance, increased development in neighbouring cities contributed to an increase in waste production, but their collection for treatment and/or disposal is still insufficient [51]. Thus, the majority of waste from restrooms, latrines, and septic tanks is thus dumped into surrounding drains before ending up in the river, which is in a low-lying location and also serves as a runoff sink [52]. In addition, the minimum temperature in winter is 10°C or lower, and the maximum temperature in April to June can reach 40°C to 46°C. This river has 65 tributaries in all, and the increased valuable contribution of underground water to ground flow indicates a risk of water logging in the basin's lower regions.

3. Data Collection and Analytical Procedures

The water samples (in 22 numbers) were collected on monthly average basis from 13 sampling sites during monsoon (July-September) for 5-year period i.e., 2018-2023 from the study area according to guidelines laid down in APHA [53]. The locations were chosen in accordance with population density. Hence, water quality data was acquired from the State Pollution Control Board (SPCB), Odisha (India). The sampling locations were marked with the help of global positioning system (GPS). Before analysis, all the glass wares were cleansed with 1:3 nitric acid and ultimately washed with a comparable water sample after using distilled water. These materials were sent to the testing site for in-depth examination after being kept in sealed, ice-cold chests at 4°C. Some of the variables comprises of electrical conductivity (EC), pH, dissolved oxygen (DO), turbidity, and total dissolved solids (TDS) were monitored on the location itself via the use of a water quality analyzer. Remaining indicators like DO, pH and EC were also determined by utilizing Winkler Azide modification approach, Systronics pH and Conductivity meter. To ascertain total dissolved solids (TDS) along with total suspended solids (TSS), Gravimetric method was employed. It is being observed that total hardness (TH) was measured by titration with Ethylenediamine tetra acetic acid (EDTA) employing Eri chrome black-T indicator. Alkalinity and Bicarbonate (HCO₃⁻) were examined by Titration procedure. Potassium (K⁺) and Sodium (Na⁺) both collectively calculated with the assistance of Systronics Flame photometer. Bioassay test was performed for measuring biochemical oxygen demand (BOD). Metals like calcium (Ca²⁺), magnesium (Mg²⁺), chromium (Cr²⁺) and iron (Fe²⁺) were examined utilizing an atomic absorption spectrophotometer. Total coliform (TC) and Fecal coliform (FC) was analyzed by counting methods (ISO 10304-1:2007). Sulphate (SO₄²⁻), Nitrate (NO₃⁻) and Phosphate (PO₄³⁻) were measured using ion chromatography. The chloride (Cl⁻) was measured using AgNO₃ titrimetric method. The quantitative parameters' units were stated in milligrams per liter (mg/L) and milliequivalent per liter (meq/L), with an exception of pH (non-dimensional) and EC conveyed in μS/cm at 25°C. When sampling and testing, 'quality assurance and quality control' are effective ways to get more precise data. The reliability of the research was governed in Eq. (1), by the Charge Balance Error (CBE), which is indicated by

$$\text{CBE} = (\sum \text{Cation} - \sum \text{Anion}) / (\sum \text{Cation} + \sum \text{Anion}) \quad (1)$$

which resulted in ± 5% concentration of major cations and anions. GIS was applied to process the data, extract clipped Landsat scenes from the delineated catchment extent, and produce change detection maps. Areas showing the various defined locations were digitized from the aerial photographs and topographic maps. Further, entropy-WQI was used to categorize water for any usage, and the spatial distribution of pollutants was used to understand the impact of urbanization. All mathematical models and calculations were performed using MATLAB software.

4. Methodology

4.1. Entropy weighted water quality index (EWQI)

In this method, objectives are first determined (decision matrix), then computations of the normalized choice matrix, probability that the attribute will occur, entropy value, average entropy contained by each explanation, and entropy weight are performed [54]. There are two possible values for information entropy (f) namely 0 and 1. This technique is computed by the subsequent equations as per [55, 56], which is represented in Eq. 2 and 3,

for efficiency type parameters,

$$Y_{ij} = (W_{ij} - W_j^{\min}) / (W_j^{\max} - W_j^{\min}) \quad (2)$$

and for cost type parameters,

$$Y_{ij} = (W_j^{\max} - W_{ij}) / (W_j^{\max} - W_j^{\min}) \quad (3)$$

where,

W_{ij} specifies the j^{th} variable value, in relation to i^{th} water sample; W_j^{\min} and W_j^{\max} specify the maximum and minimum value of the respective indicator. Values for the index ratio of j index in i samples were calculated using Eq. (4).

$$X_{ij} = (W_{ij} + 0.0001) / \sum (W_{ij} + 0.0001) \quad (4)$$

The index value ratio of X_{ij} exhibits as the ‘overall sample entropy information’, denoted e_j for the j^{th} parameter, is calculated in Eq. (5).

$$e_j = (1/\ln m) \times \sum X_{ij} \times \ln X_{ij} \quad (5)$$

At this point, the entropy weight can be determined in Eq. (6).

$$A_j = (1-f_j) / \sum (1-f_j) \quad (6)$$

The quality rating scale (U_i) has been calculated using Eq. (7).

$$U_i = (O_j/M_j) \times 100 \quad (7)$$

The variable O_i is a variable that measures water quality and expressed in the form of a variable ‘ j ’ (mg/l) and M_j exhibits about the desirable boundaries set by WHO Standard (in mg/l).

The EWQI has also been determined in Eq. (8)

$$EWQI = \sum A_i \times U_i \quad (8)$$

For checking the accuracy, the quality grading scale of the suggested index proposed using [57, 58] that symbolizes water is of excellent quality if the EWQI is less than 50, good if the EWQI is between 50 and 100, average if the EWQI is between 100 and 150 and ultimately, poor if the EWQI is greater than 200.

4.2 Technique for Order of Preference by Similarity to Ideal Solution (TOPSIS)

This strategy, which is created on statistical entropy, seeks to find an alternative option that is closest to the positive ideal solution (PIS) and most distant from negative ideal solution (NIS) by determining their Euclidean distances [59]. Depending on user-defined parameters and entropy weights, TOPSIS approximates a weighted normalized matrix in the light of uncertainty.

The following equation Eq. (9), as suggested by [60], which yields the normalized decision matrix (NDM), which represents a comparison of the options' performance and it is denoted as

$$\text{NDM} = r_{ij} = a_{ij} / (\sum a_{ij}^2 + \dots + a_{mj}^2)^{0.5} \quad (9)$$

A weighted normalized decision matrix was created in Eq. (10) and it is expressed as

$$Y = N_{m \times c} \times [r_{ij}]_{m \times c} \quad (10)$$

The following criteria weights were calculated using information entropy approaches and illustrated in Eq. (11) and depicted as

$$v_{ij} = (a_{ij}/a_{1j} + \dots + a_{mj}) \text{ for all } j \in \{1, \dots, c\} \quad (11)$$

$$L_j = (-1/\ln m) \times \sum p_{ij} \ln p_{ij}; \text{ for all } j \in \{1, \dots, c\}.$$

The value of L_j lies between 0 and 1. In contrast, the fluctuation in the index with higher entropy is bigger. Consequently, the criteria's weight in Eq. (12), can be determined as

$$w_j = (k_j/k_1 + \dots + k_c) \text{ and } k_j = 1 - L_j \quad (12)$$

Further, the considered 'weights' were combined to produce a grid $w_{c \times c}$. The alternatives' PIS and NIS were determined in Eq. (13)

$$\text{PIS} = \{\max p_{ij} \mid p_{ij} \in Y\} = (p_1^+, \dots, p_c^+) \quad (13)$$

$$\text{NIS} = \{\min p_{ij} \mid p_{ij} \in Y\} = (p_1^-, \dots, p_c^-)$$

The Euclidean distance in Eq. (14), between each possible choice within the PIS (k_i^+) and NIS (k_i^-) were evaluated as:

$$k_i^+ = (\sum (p_{ij} - p_j^+)^2)^{0.5} \text{ and } k_i^- = (\sum (p_{ij} - p_j^-)^2)^{0.5} \quad (14)$$

Each alternative's proximity coefficients (CC) were calculated in the manner described in Eq. (15)

$$\text{CC}_i^+ = d_i^-/d_i^- + d_i^+ \quad (15)$$

Eventually, the possibilities were ordered based on their closeness coefficients [61].

5. Results and Discussions

Statistical overview of the surface water parameters in the area under examination are demonstrated in the following Table 1. The pH of each sample that was taken spanned from 6.44 to 7.43 and is reported to be marginally alkaline. This could be related to the discharge of wastewater and the leakage of textile effluents [62]. Acidic pH at St. 2, 7, 8, 10 and 12 depletes calcium, magnesium, and potassium, all of which are necessary for plant growth. The current readings were within the acceptable range (6.5 to 8.5). Turbidity is highly essential aesthetic tool to quantify the water's clarity or cloudiness [63]. The upper limit that is permitted in water is taken as 5 NTU. The turbidity of the samples collected that were obtained fluctuates between 18.7 and 65.4 NTU, indicates that the results are above the WHO guidelines in all stations. Freshwater that is murky and turbid may be due to microscopic particles, usually clay along with silt, also contains fine organic and inorganic compounds, dissolved pigmented organic materials, algae, and other substances. Agriculture operations, residential runoff, soil contamination brought on by leaching, and point

source water pollution discharged from corporate or municipal treatment plants are the primary causes of TDS.

Table 1. Comprehensive overview of water quality parameter and a comparison to WHO guidelines

Variables	Minimum	Maximum	Standard Deviation (S.D.)	WHO (2017)
pH	6.44	7.43	0.30	8.5
Turbidity	18.7	65.4	12.41	5
TDS	98	218	42.37	500
TSS	85	168	25.16	500
EC	108	372	74.36	2250
DO	5.87	7.87	0.61	5
Alkalinity	43	95	17.05	120
BOD	1.05	5.16	1.10	5
TH	64	119	17.45	300
HCO ₃ ⁻	45.83	74.31	8.57	100
SO ₄ ²⁻	2.26	5.19	0.91	250
NO ₃ ⁻	1.31	5.3	1.37	45
PO ₄ ³⁻	0.22	1.18	0.28	1.2
Cl ⁻	7.3	22.12	4.68	250
Ca ²⁺	12.83	25.35	3.68	75
Mg ²⁺	0.97	5.11	1.26	50
Na ⁺	2.9	10.7	2.43	200
K ⁺	1.2	3.7	0.79	12
TC	3000	15000	3058.22	1000
FC	150	590	135.41	300
Fe ²⁺	0.171	0.658	0.15	1
Cr ²⁺	0.053	0.194	0.04	0.5

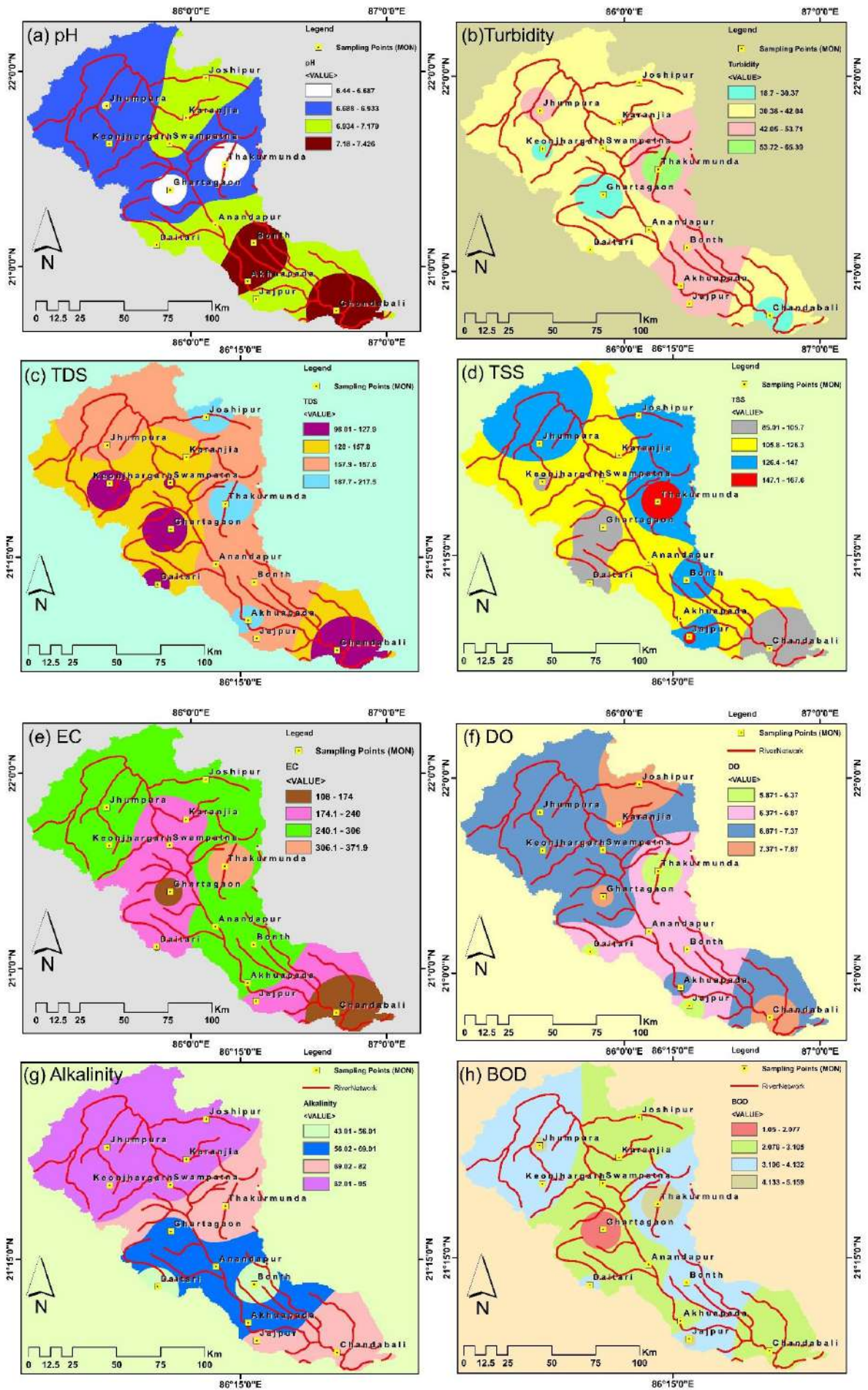
Information gained from the ongoing work, its readings swing between 98 to 218 mg/l. Nonetheless, all of these sample collection results come well within the TDS cutoff limitations set by the WHO (i.e., < 500 mg/l). It is clear that EC represents the ability of water to conduct electricity and it depends on ion concentration in the water. Although crop growth phase fluctuates with soil mineral assimilation, having too much of it in irrigation water could have an impact on crop productivity. In this inquiry, The EC rates at each area vary from 108-372 $\mu\text{S}/\text{cm}$, which are within the expected range of 2250 $\mu\text{S}/\text{cm}$. On the other hand, irrigation water is rated as excellent, which consists of $\text{EC} < 250 \mu\text{S}/\text{cm}$, from 250 to 750 $\mu\text{S}/\text{cm}$, it depicts good water. While between 750 and 2250 $\mu\text{S}/\text{cm}$, it belongs to permissible, if appropriate management is offered [64]. As a result, the current data demonstrated that all sampling stations' water quality, as measured by EC, qualified into the good category. The samples' DO levels were found to be within the range of 5.87-7.87 mg/l. It is seen that DO was healthy in all sampling locations.

Alkalinity is defined as a gauge of the buffering potential of water. In drinkable water, 120 mg/l is the recommended limit, beyond which the aroma of the water turns unpalatable. Within the survey area, the concentration contains around 43 to 95 mg/l, which is well fit into the acceptable boundary. BOD is an indicator that estimates how much oxygen is used by microorganisms in the aerobic decomposition of organic materials in water. It was positioned between 1.05-5.16 mg/l. The acceptable BOD for consuming and drinking water is 5 mg/l [65]. The results are within the acceptable limits. Higher value at St-8, indicates high concentration of organic contaminants. Water Hardness is caused primarily by the presence of cations such as Ca²⁺ and Mg²⁺ and anions such as CO₃²⁻, HCO₃⁻, Cl⁻ and SO₄²⁻ in water [66]. The values in the investigated region ranged between 64-119 mg/l. Each sample is much below the allowed level of 300 mg/l. In the research area, HCO₃⁻ is the dominant anion. According to [67] declared that HCO₃⁻ significant values

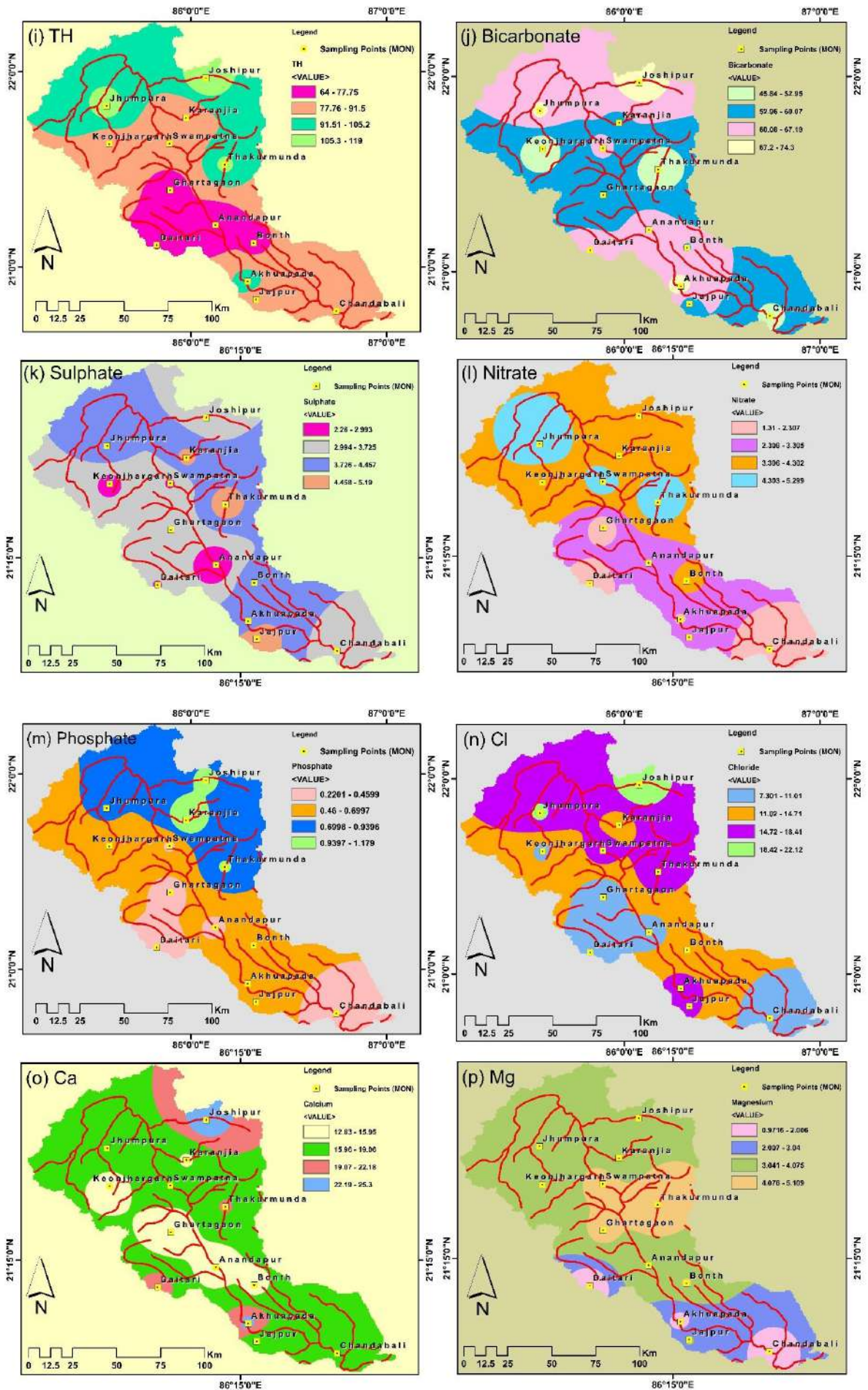
in surface water may result from the interaction between dissolved CO_2 and acidified volcanoes. The concentration ranges from 45.83-74.31 mg/l. According to the criteria established by WHO of 100 mg/l, all samples are suitable for drinking purposes. Increase in SO_4^{2-} might be related to industrial farming runoff as the location come under vigorous activity focused on agriculture [68]. On high values, it causes gastrointestinal pain and has an antidiarrheal effect on people. However, in the ongoing research, the value (2.26-5.19 mg/l) in all sites are below the WHO guideline' normal limit. Increased NO_3^- concentrations were linked to the breakdown of organic matter from domestic wastes, sewage, and animal wastes, along with nitrogen fertilizer, they are essentially a sign of anthropogenic activities [69]. The value in the present study ranged from 1.31-5.3 mg/l. Nearly all of the data are far below the WHO-recommended permissible nitrate threshold of 45 mg/l.

Untreated industrial effluents that contain humans and other animals waste can discharge a lot of PO_4^{3-} into the surface water. On account of higher degree, it could explain the higher density of plants [70]. In the research study, PO_4^{3-} concentration is low and ranges between 0.22-1.18 mg/l, satisfying nicely inside the WHO criteria of 1.2 mg/l. Drinking water may have a salty flavour if there is too much Cl^- in the surface water. Elevated Cl^- concentrations are hazardous to plants, which impact plant function and lower productivity as a result of reduced soil permeability [71]. In the period of survey, the concentration spanning from 7.3-22.12 mg/l, that comes under the WHO's range of 250 mg/l. Ca^{2+} along with Mg^{2+} are important elements for plant growth [72]. When calcium levels are high, major health issues such kidney stones and cardiovascular diseases occur. Ferromagnesium minerals and household waste waters are the reliable sources of Mg^{2+} within surface water. Furthermore, accumulation of Mg^{2+} supports the plant's uptake of nutrients i.e., Ca^{2+} or K^+ in the irrigated water, which account for their lack of plant tissue. In this study, Ca^{2+} and Mg^{2+} values ranged from 12.83-25.35 mg/l and 0.97-5.11 mg/l respectively. However, in case of drinking water, the value should not exceed 75 mg/l and 50 mg/l respectively. All detected locations are within the guidelines. Excess Na^+ amount lowers the amount of water that can be absorbed by the soil, which can cause excessive weed growth, seed rot, and an obstruction in the flow of water to the roots [73]. The current reading of Na^+ ranged from 2.9-10.7 mg/l. However, all levels are within the range when contrasted to drinking and irrigation water quality guidelines. Chemicals applied on farmland emits K^+ , when there is irrigation and rains This load is transported by runoff to the accessible surface water body, causing agricultural non-point source pollution. The reported readings found to be in a span of 1.2-3.7 mg/l. Threshold limits taken as 12 mg/l. However, the parameter was safe for all sites in case of drinking and irrigation criteria.

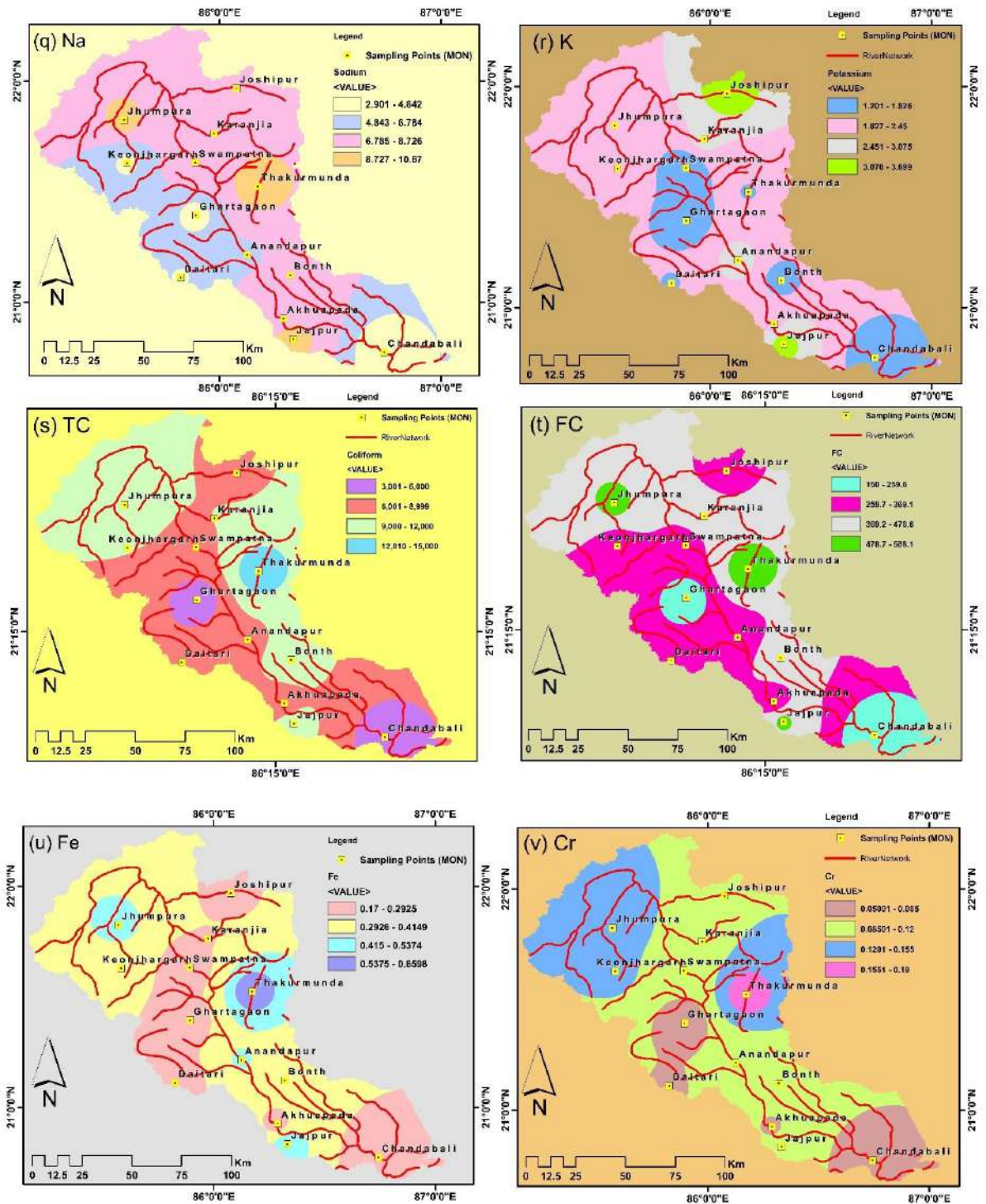
Due to water pollution, it leads to the formation of high TC and FC coliforms in surface water. Because of high temperature, these coliforms lead to the growth and multiplication of bacterium. Recorded values of TC and FC in the present study ranged from 3000-15000 and 150-590 respectively. The quantities of coliform are larger in most of the sites because, these areas are adjacent to sewage expulsion or industries. Similar to this, waters near factories, municipal sewage systems, or hospitals have been demonstrated to contain much substantial quantities of coliform bacteria. Severely rise in E coli and fecal coliform counts, might be injurious to agriculture production and human health [74]. Although Fe^{2+} is a crucial component needed for bringing oxygen into the blood, nonetheless, it has the ability to harm DNA and cause hemochromatosis at high concentrations. Greater concentration of Fe^{2+} can trigger fatigue, lose some weight, joints ache, stomach issues and vomiting [75]. The mean proportion in the ongoing study of Fe^{2+} was reported to 0.32 mg/l. These readings were eventually lower than the stated allowable limits by (1 mg/l) [65]. Cr^{2+} often takes place in the divalent state, yet there may also be trivalent oxidation states in natural [56]. Generally, this metal is hazardous to public health and may have its harmful consequences on people residing nearby. In this study area, the value ranged from 0.05-0.19, which is within of the permissible limits of WHO. Finally, during monsoon season, the sequence of the major cations adhering to the norms as $\text{Ca}^{2+} > \text{Na}^+ > \text{Mg}^{2+} > \text{K}^+$, while in case of anions, its sequence of path is $\text{HCO}_3^- > \text{Cl}^- > \text{SO}_4^{2-} > \text{NO}_3^-$. Figure 2a-v display a reconstructed map of the periodic and geographic shifts of all elements relevant to the study.



(a) pH, (b) Turbidity, (c) TDS, (d) TSS, (e) EC, (f) DO, (g) Alkalinity and (h) BOD



(i) TH, (j) HCO_3^- , (k) SO_4^{2-} , (l) NO_3^- (m) PO_4^{3-} , (n) Cl^- , (o) Ca^{2+} and (p) Mg^{2+}



(q) Na⁺, (r) K⁺, (s) TC, (t) FC, (u) Fe²⁺ and (v) Cr²⁺

Fig. 2. Spatial and temporal interpretations

The EWQI map uses ArcGIS 10.5 to prepare it based on the well determined quality criteria to distinguish between the different classes at each hydro-station for drinking purposes. The map amply demonstrates that the grade of surface water corresponds to excellent to poor category regarding its suitability for human utilization. The current studies determined values ranged between 46.11 and 198, as shown in Table 2 and its variation is being depicted in Figure 3. A minimal value of EWQI symbolizes excellent quality while a greater score suggests poor quality. As represented in Table, 15.38% of the overall water samples belongs to excellent zone. 38.46% samples fit into good water class. Unfortunately, remaining 30.77% of the water samples representing the sites namely St-8, 11, 12 and 13, had water that shows poor water quality and, finally, none of the samples included water that was not fit for drinking. Similar to this,

15.38 percent of the samples from sites St-9 and 10 indicate medium water quality according to the EWQI categorization. Sites detected in excellent, good, and medium class of water, represents the population density is considerably lower, and there are less people living there. St-1 and 2 indicated water quality as excellent. It shows how the river is assimilating itself. Stronger EWQI readings was noticed at poor sampling locations, which are situated close to the crowded market area and also, receives pollutants from domestic water. The high amounts of TC and turbidity were the main factors for such a high EWQI. Overall, the quality of surface water belongs to good category (38.46%) in a significant percentage of the research area and is potable and residential use.

After that, geostatistical techniques were used to interpolate the obtained values, to highlight areas, comprised of good, medium, excellent, and poor water qualities. The parameters used for the EWQI calculation were also employed for the TOPSIS analysis to obtain additional information about the surface water quality of the entire river watershed. The data frame applied for interpretation comprised of 13 monitoring stations and 22 variables (factors used for EWQI calculation). The performance/closeness coefficient value in the ongoing study spanning from 0.17 to 0.78 (Table 2). The present investigation has witnessed at St-8, as the most polluted site on the basis of highest performance value (C.C = 0.78) and allotted 1st rank followed by 2nd (St-12), and 3rd (St-13), because of maximum efficacy of total impacts of combined manmade accompanied with ecological practices affecting water quality, existence of communities and industries, heavy metals may be getting in through sporadic factory wastewater output and also from a wide range of manufacturing industries. The major parameters involved at these sites is Coliform, which in water, has sanitary contamination as its source and also turbidity, which arises from farmland runoff, sewerage, pesticides, and the petrochemical industries. The placement of the sample sites (Figure 3) focused on the specified entropy-based water quality categories is comparable to what was previously discussed but the TOPSIS scores provide perspective into the EWQI framework. Figure 4 (a, b) shows the variations of EWQI and TOPSIS of all sampling locations.

Table 2. Computed EWQI and TOPSIS with each water sample during monsoon season

Station Code	EWQI value	Type of water	Closeness	
			coefficient (CC)	Rank (TOPSIS) score (TOPSIS)
St. 1	46.11	Excellent	0.175	13
St. 2	48.73	Excellent	0.514	5
St. 3	71	Good	0.427	8
St. 4	78	Good	0.240	11
St. 5	72	Good	0.504	6
St. 6	91	Good	0.400	10
St. 7	87	Good	0.209	12
St. 8	198	Poor	0.782	1
St. 9	143	Medium	0.431	7
St. 10	148	Medium	0.408	9
St. 11	157	Poor	0.585	4
St. 12	162	Poor	0.667	2
St. 13	182	Poor	0.589	3

EWQI & TOPSIS Map for Baitarani Basin, Odisha

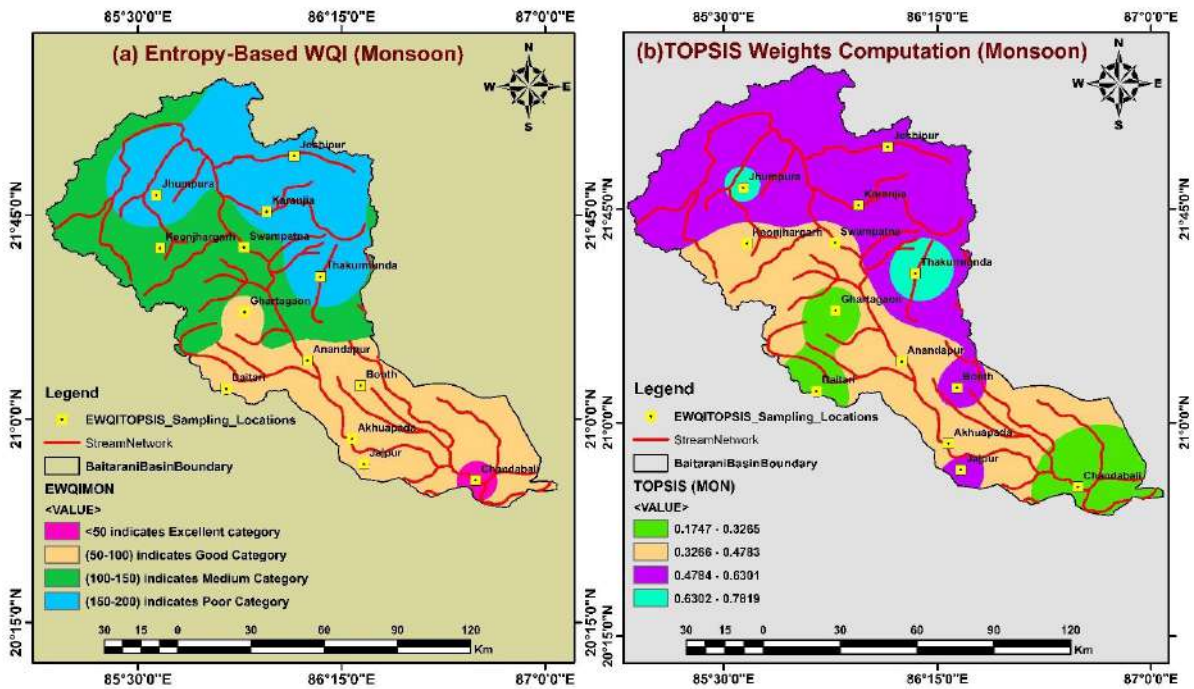


Fig. 3. Spatial variations in surface water quality based on EWQI and TOPSIS method

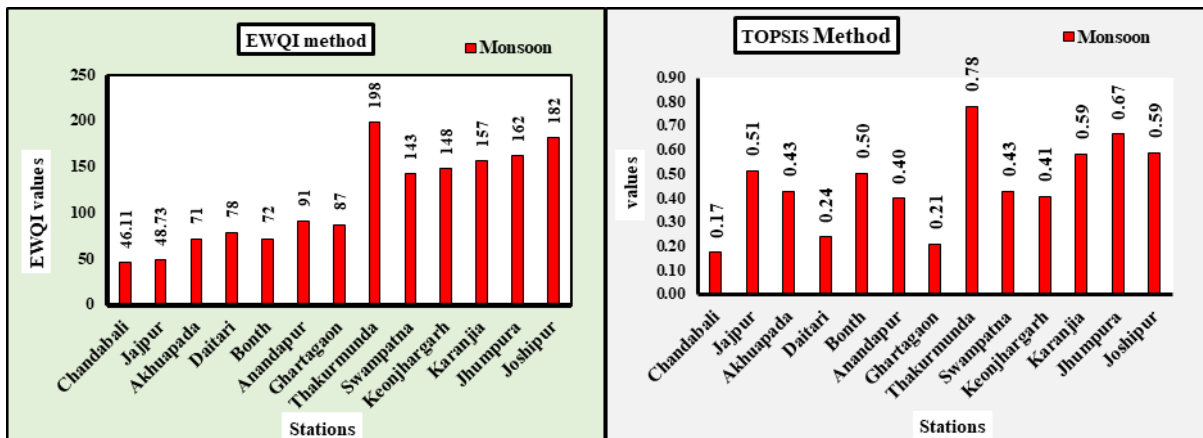


Fig. 4. Bar plots of (a) EWQI and (b) TOPSIS approach

5.1. Suitability for irrigational uses

According to our information, agriculture practices, soil types, and water quality play a part in deciding on the best irrigation techniques [76]. So, numerous indices were used to keep an eye on the water quality for agricultural use featuring Kelley’s index (KI), Magnesium hazard (MH), Potential salinity (PS), Residual sodium carbonate (RSC), Sodium adsorption ratio (SAR), Permeability index (PI), Chloroalkaline indices 1 (CAI1), Corrosivity ratio (CR), and Chloroalkaline indices 2 (CAI2) concerning irrigation. These strategies rely the potential risk of salinization of soil. In addition, it has a detrimental effect on plants and soils. In Equations 16-24, the agricultural indices may be calculated, which is given by:

$$\text{SAR} = \text{Na}^+ / [(\text{Ca}^{2+} + \text{Mg}^{2+})/2]^{1/2} \quad (16)$$

$$\text{RSC} = (\text{CO}_3^{2-} + \text{HCO}_3^-) - (\text{Ca}^{2+} + \text{Mg}^{2+}) \quad (17)$$

$$\text{MH} = [\text{Mg}^{2+} / (\text{Ca}^{2+} + \text{Mg}^{2+})] \times 100 \quad (18)$$

$$\text{KI} = \text{Na}^+ / (\text{Ca}^{2+} + \text{Mg}^{2+}) \quad (19)$$

$$\text{PS} = \text{Cl}^- + (0.5 \text{SO}_4^{2-}) \quad (20)$$

$$\text{CR} = [(\text{Cl}^-/35) + \{2(\text{SO}_4^{2-}/96)\}] / (\text{CO}_3^{2-} + \{\text{HCO}_3^-/100\}) \quad (21)$$

$$\text{CAI1} = (\text{Cl}^- - \{\text{Na}^+ + \text{K}^+\}) / \text{Cl}^- \quad (22)$$

$$\text{CAI2} = (\text{Cl}^- - \{\text{Na}^+ + \text{K}^+\}) / (\text{SO}_4^{2-} + \text{CO}_3^{2-} + \text{NO}_3^-) \quad (23)$$

$$\text{PI} = \{[\text{Na}^+ + (\text{HCO}_3^-)^{1/2}] / (\text{Ca}^{2+} + \text{Mg}^{2+} + \text{Na}^+)\} \times 100 \quad (24)$$

In case of Sodium adsorption ratio (SAR), Na^+ ions in the irrigation water might hinder plant growth by altering the soil's aeration, permeability, alkalinity, and texture [77]. SAR values have been calculated for the research region using Eq. 16, that differ in values, from 0.13 to 0.41 meq/L. The classification addressed by [78], which tells about the core for the suggestion that samples of surface water are grouped as excellent. However, the investigated map drawn in Figure 5a, showed that all analysed samples possess an extremely low risk of alkalinity in the study region. Intricate information on the insight in contrast to SAR is generated from United States salinity diagram [79]. It was found from Figure 6, that most of the samples belongs to C1- S1 class, which represents low salinity and low alkalinity danger. Few comes under C2-S1, that belongs to medium salinity and low alkalinity region.

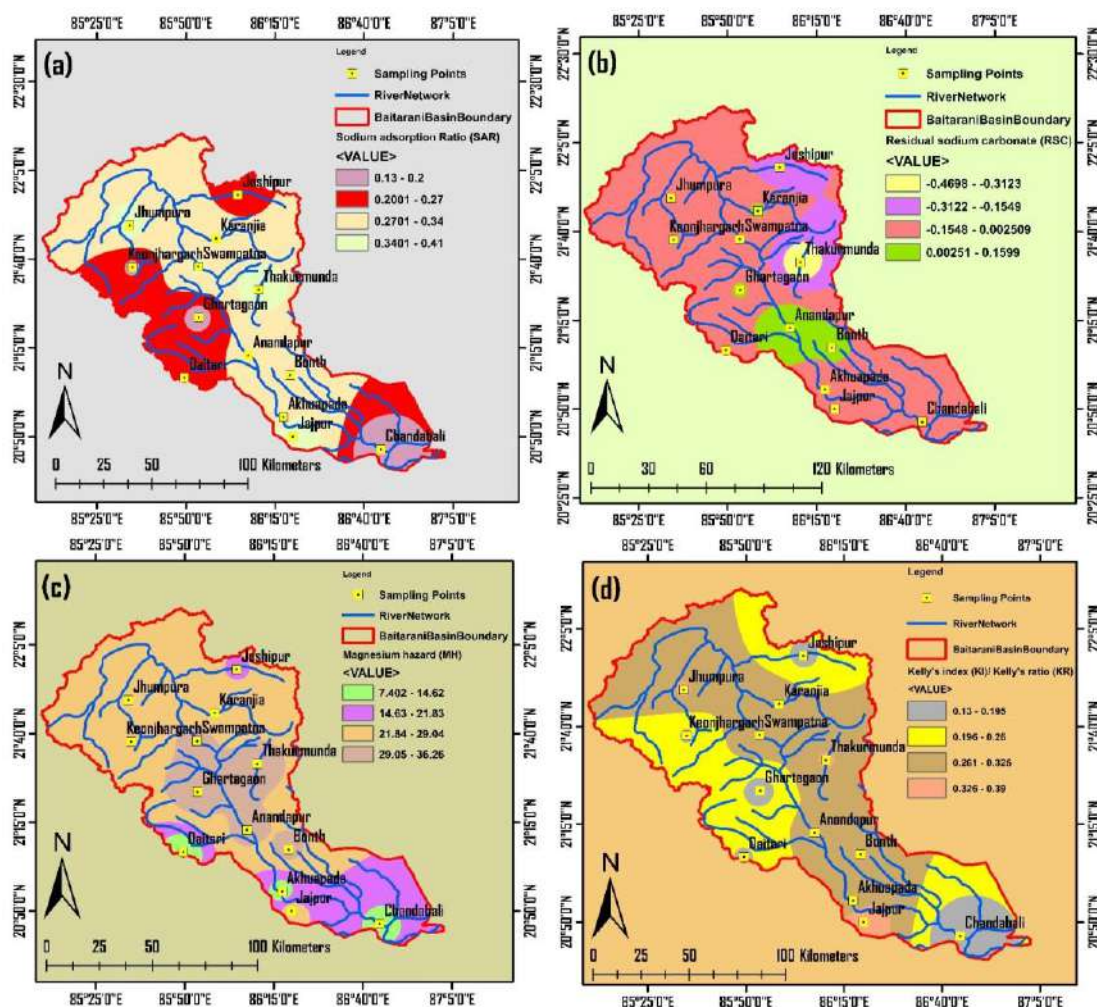


Fig. 5. Spatial and temporal variations of (a) SAR, (b) RSC, (c) MH, and (d) KI in monsoon season

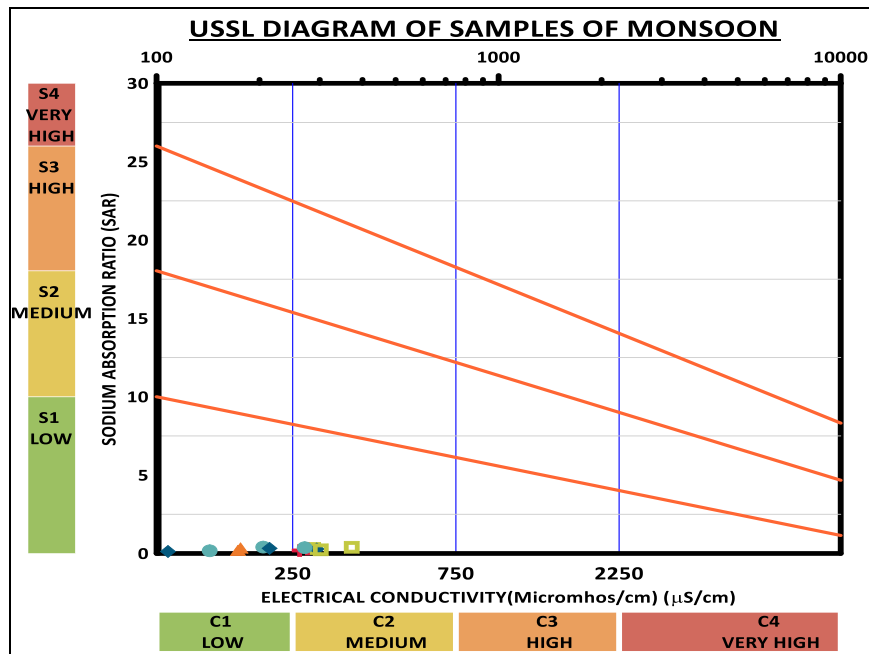


Fig. 6. USSSL salinity diagram showing classification of surface water in monsoon season for irrigation purposes

Because Ca^{2+} and Mg^{2+} are accelerated by high HCO_3^- concentrations, RSC determines the requirement of irrigation water. In the subsequent pattern of NaHCO_3 , the relative fraction of Na^+ is also increased [80]. Concentration value of lesser than 1.25 meq/L is termed as good, while in between 1.25 and 2.5 meq/L score, it represents doubtful for irrigation activities. Moreover, in water, with an RSC greater than 2.5 meq/L, it is often called as unsuitable. In this research, the RSC value in all sites is being determined using (Eq. 17) and the value found in a range of -0.47-0.16 (Figure 5b). This finding highlighted that the entire area has very little RSC, and it is considered as suitable. Negative value arises in RSC, which could be due to a variety of dissolved ions, minerals, and inorganic particles from household garbage. The MH index from (Eq. 18) is used to Identify the effects of Mg^{2+} in agricultural water, which is being suggested by [81]. The majority of natural waters maintain an equilibrium calcium and magnesium concentration; however, they act differently in soil ecosystem (Subba Rao 2017). The danger of $\text{Mg}^{2+} > 50\%$ is averse to crop harvests (Berhe 2020). During the sampling period, the ratios were 7.39-36.26 (Figure 5c).

According to research, river water can be used for agriculture. From (Eq. 19), KI assists with determining the cumulative exchangeable Na^+ proportion. $\text{KI} > 1$ indicates that the water is not adequate to use and possess an extra concentration of sodium in waters whereas KI value less than 1 specifies that it can be used for irrigation and $\text{KI} < 2$ imply surplus Na^+ and sodium insufficiency in water [82]. In the study region, water sites were reported to be in a range of 0.13-0.39 (Figure 5d), thereby signalling that water is acceptable for agriculture. It could also be because of prevailing levels of Ca^{2+} and Mg^{2+} throughout each water sample, and consequently, the water in these locations is suitable for irrigation. The PS of surface water is compelled by the composition of Cl^- and $\frac{1}{2}$ of SO_4^{2-} value using Eq. 20 [83]. Surface water can be divided into four groups based on PS readings and it suggests excellent to good (< 3), good to injurious (3-5) and finally, injurious to unsatisfactory (> 5). The PS levels ranged from 0.22 to 0.64 meq/L, according to the findings. It is noticed that the value is < 3 meq/L, indicating in (Figure 7a), that 100% of water samples are identified as excellent-good.

A key determinant called to be corrosivity ratio (CR), which refers as a vital indicator that decides that the water might be transported using a metal pipe. From Eq. 21, if the readings of CR are lower than 1, then it implies that we may supply water through a metal pipe, whereas when CR value > 1 , it signifies using a metal pipe to supply water is not recommended. It is owing to higher corrosion. The current analysis

revealed that the CR level across all sites recorded a score between 0.50-1.31 mg/L (Figure 7b). Elevated CR value at St-8 is attributed to larger Cl^- and SO_4^{2-} concentrations in drainage water [84]. The prominent indicator named as Chloroalkaline index (CAI), that refers to be a result of the rise of chloride ion. Generally, Cl^- influences soil chemistry and also it supports plant photosynthesis [85]. It can be obtained from Eq. 22 and 23. In this study, as seen in (Figure 7c, d), CAI-1 and CAI-2 were found to be -0.33-0.37 and -1.48-2.34 meq/L, respectively. So, both CA-1 and CAI-2 readings found to be positive, demonstrating a straight interaction between K^+ and Na^+ ion in water, which is also associated with Ca^{2+} and Mg^{2+} from rock. So, negative value containing sites, which signifies normal ion exchange process.

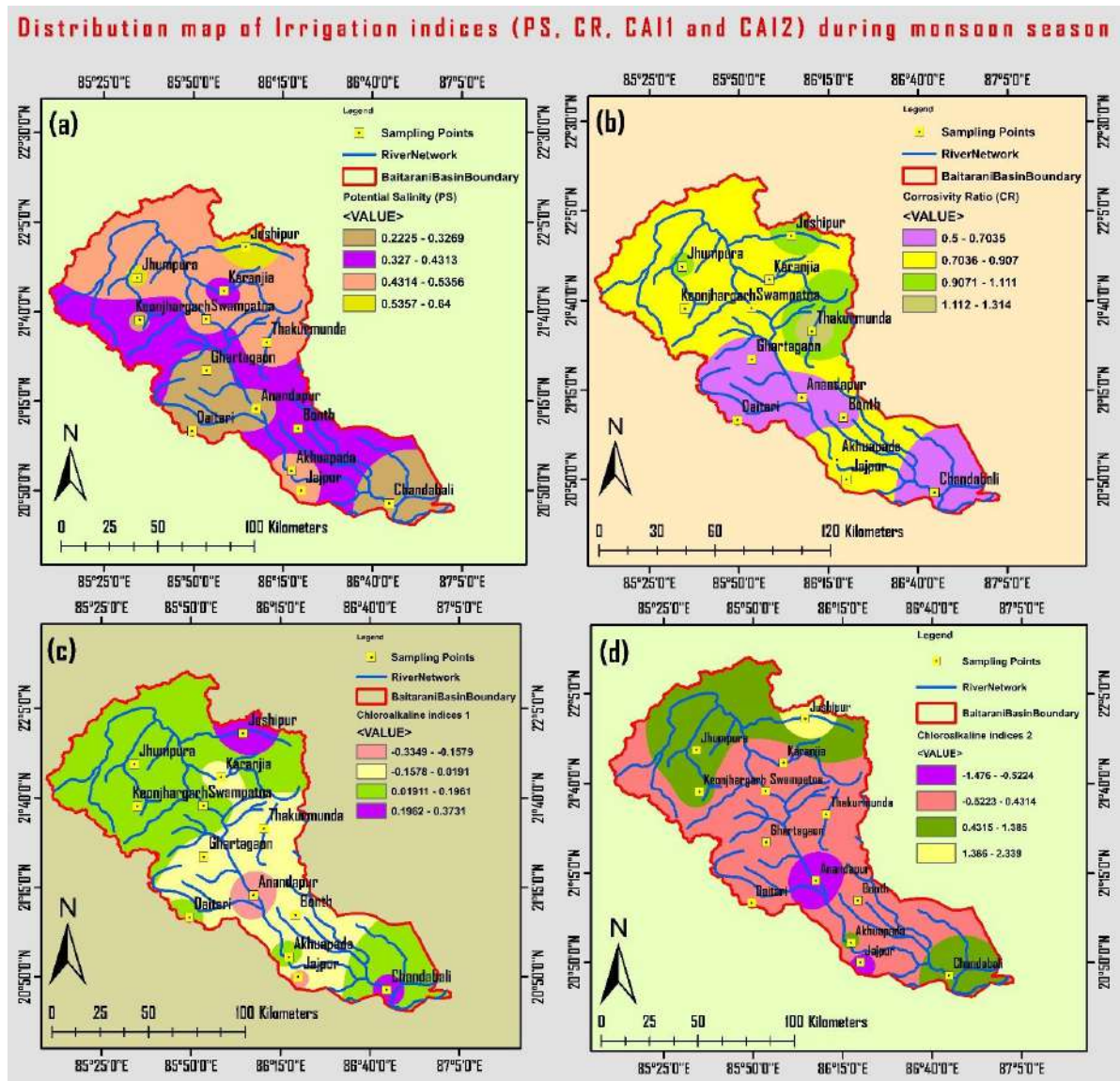


Fig. 7. Spatial and temporal variations of (a) PS, (b) CR, (c) CAI1 and (d) CAI2 in monsoon season

The long-term usage of irrigation water, which is regulated by the ions Na^+ , Ca^{2+} , Mg^{2+} , and HCO_3^- affects the soil permeability [86]. According to permeability, [87] listed the water designs as (PI less than 75%) as ‘beneficial’ for irrigation due to its maximal permeability (Class I). On the other hand, Class II refers to a PI value of 25-75%, which talks about ‘moderately suitable’ and finally, the ultimate group i.e., Class III records a score of $\text{PI} < 25\%$, which appraise unsuitable irrigation water, since they contain less permeability. Based on PI values using Eq. 24, represented in (Figure 8), it ranges from 38-63% at all sampling sites. Hence, they fall under class II, signifying the water is moderately permeable.

Distribution map of Permeability Index (PI) during monsoon season

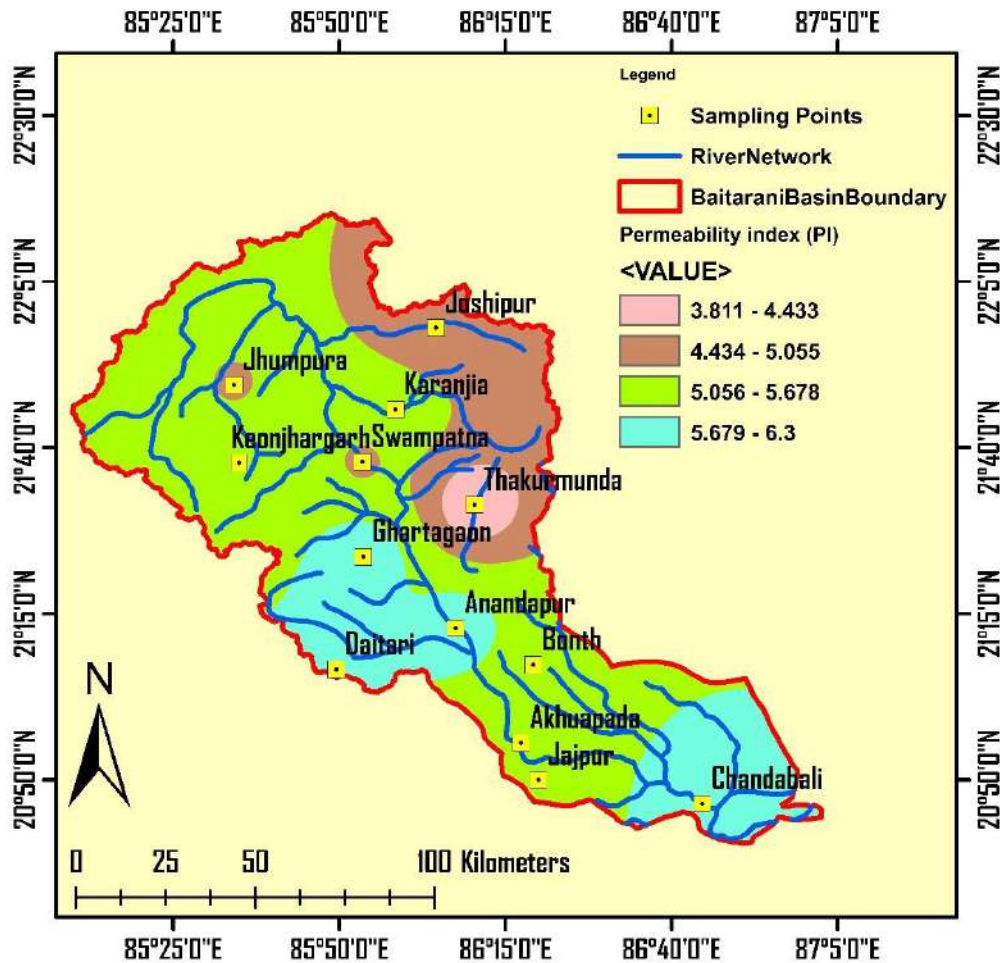


Fig. 8. Spatial variations in surface water quality based on PI values

The degree of salinization in the surface water can indeed be categorized taking Cl^- ion divided by HCO_3^- proportion. Based on classification [88, 89], < 0.5 indicates not affected zone, between 0.5 to 6.6 signifies slightly to moderately affected and finally, > 6.6 belongs to severely affected category. It was estimated in the present study for all surface water samples, the value varied from 0.13-0.38. 100% of the measurements accompanying the study area (Figure 9) encompasses values less than 0.5 $\text{Cl}^-/\text{HCO}_3^-$ ratios, they addressed that they are not harmed by salinization.

The paradigms developed by [90] aid in the analysis of evolutionary tendencies and hydro chemical processes that take place in the surface water system and can be used to denote the mixing of various water types as well as ion exchange and reverse ion exchange processes. Figure 10 observed that the water type present in the study area is found to be Na^+-Cl^- and a mixture of $\text{Ca}^{2+}-\text{Mg}^{2+}-\text{Cl}^-$ class. It demonstrates the blending of two processes clearly, suggests the appearance of Cl^- and Ca^{2+} as the main water types, and illustrates the mechanism by which salty water enters fresh water [91]. Piper diagram explains the volatility or dominance of the cation and anion amounts in clear language [92]. In the current work, the cationic triangular field suggests that calcium type represents the majority of the samples. Inside the anionic triangle, samples come under HCO_3^- class. However, all samples correspond in the category of diamond-shaped field which signifies the imbalance of $\text{Ca}(\text{HCO}_3)_2$ type. As seen in (Figure 11), after a brief period of gentle heating, water can be utilized for drinking and household tasks.

Distribution map of Salinization Ratio (Revelle 1941) during monsoon season

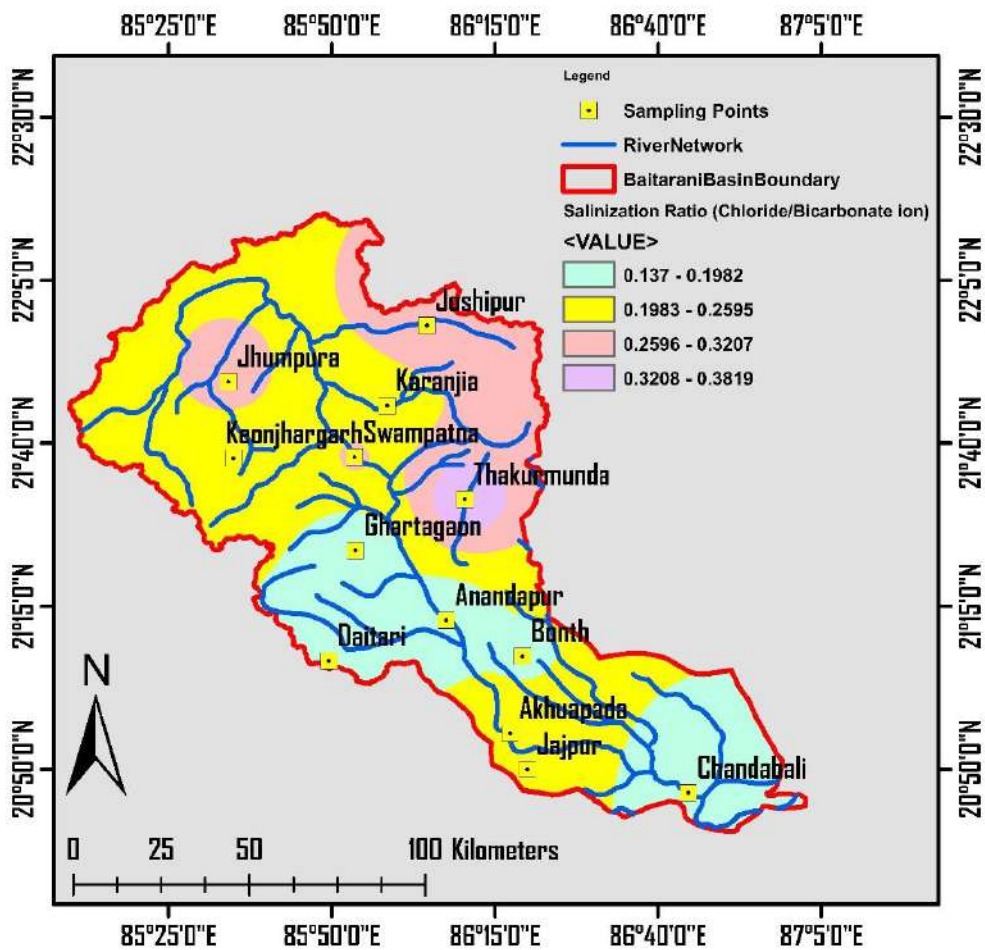


Fig. 9. Spatial variations in surface water quality based on Cl-/HCO₃- values

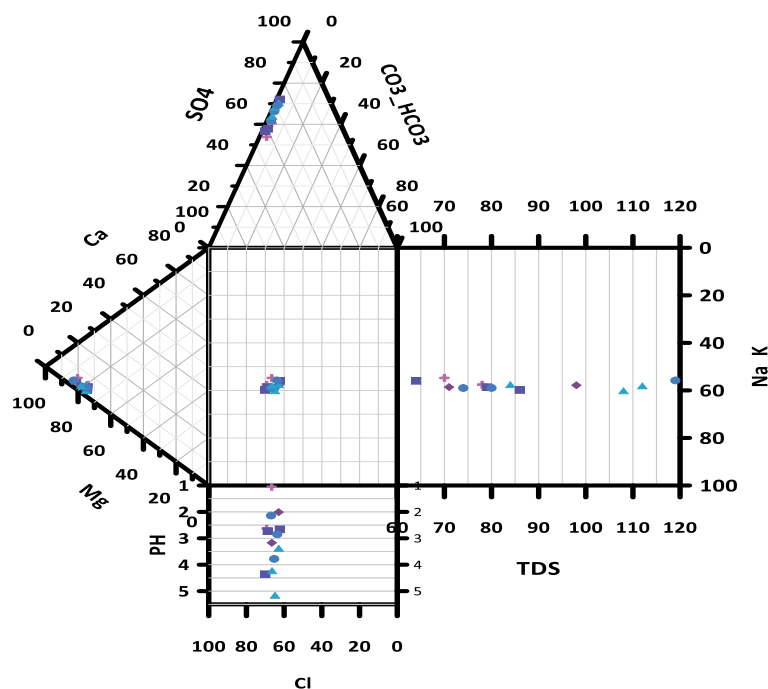


Fig. 10. Durov diagram portraying the hydro chemical facies of surface water during monsoon season

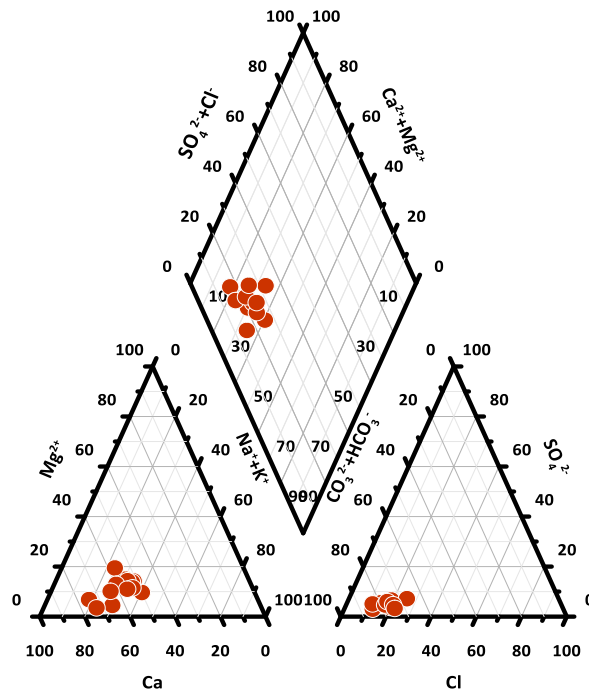


Fig. 11. Piper trilinear diagram displaying the hydro chemical facies of surface water during monsoon season

To examine hydro-chemical processes namely, rock weathering dominance, atmospheric precipitation dominance and evaporation-crystallization dominance, a Gibbs chart has been employed [93]. This is done by the weight ratios of $(\text{Na}^+ + \text{K}^+)$ divided by $(\text{Na}^+ + \text{Ca}^{2+})$ and $(\text{Cl}^- / (\text{Cl}^- + \text{HCO}_3^-))$ gets plotted in the chart and gets recognized as a byproduct of variable i.e., TDS [94, 95]. According to Figure 12, 74.23 % has a point mark in the evaporation-precipitation field. Remaining sites are influenced by rock weathering. By increasing Na^+ and Cl^- concentrations in response to an increase in TDS, evaporation raises salinity [96, 97, 98, 99]. The area under examination is classified as a semi-arid zone with below-average rainfall, making evaporation a dominating factor in determining the chemistry of the surface water. In Figure 13, consequently, the high concentrations of Na^+ and Ca^{2+} reflect rock-water interaction, while the high contents of Cl^- and SO_4^{2-} revealed saltwater intrusion. These findings might be explained by evaporation, weathering, saltwater intrusion, freshening, and rock-water interaction. Therefore, incorporating physiochemical features for surface water quality evaluation is a useful and versatile technique with exceptional potential and novel insights.

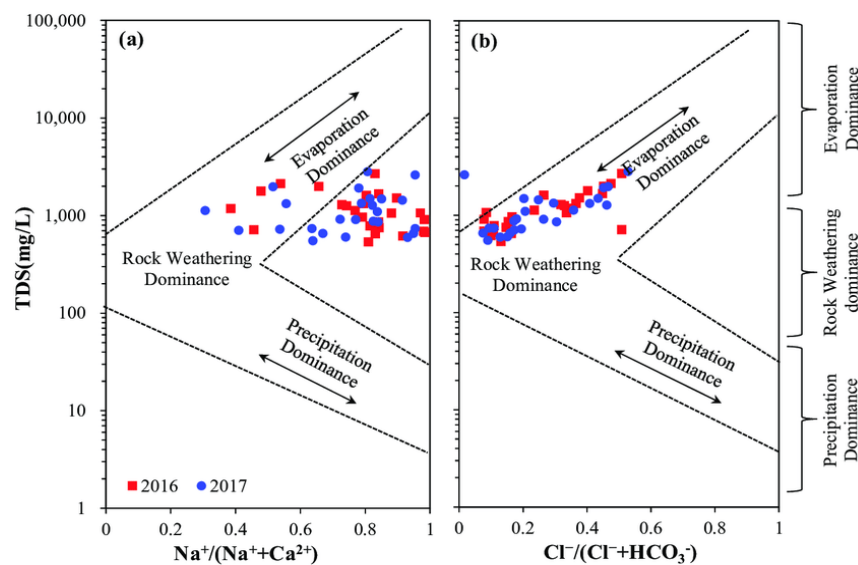


Fig. 12. Gibbs diagram showing the controlling factors of surface water during monsoon season

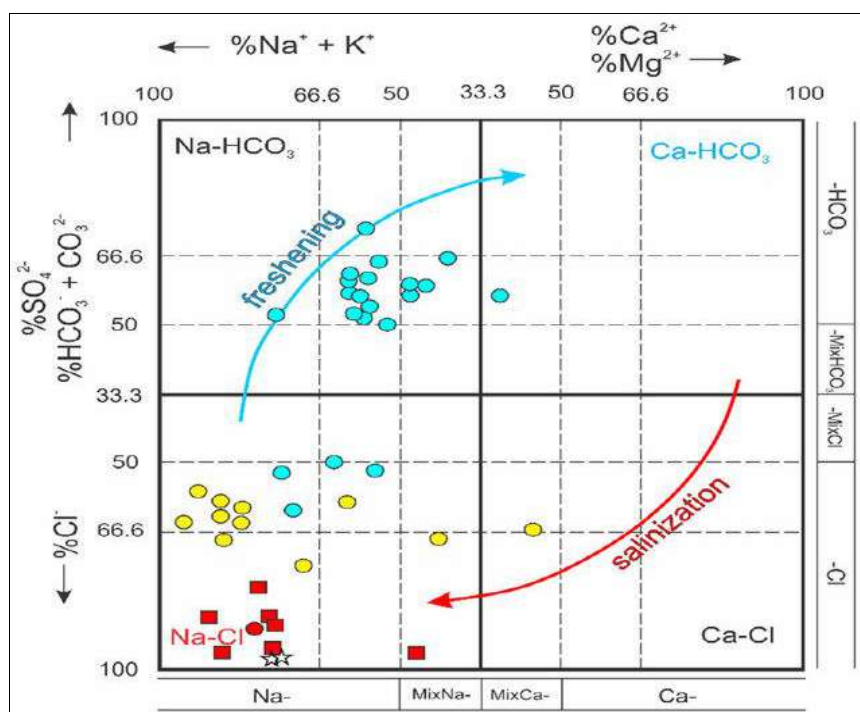


Fig. 13. Ion exchange diagram in the study region of all sample sites

6. Conclusions

Water quality is affected by area, population, and certain characteristics. Due to rising population and increased demand on water resources, the study area is constantly under pressure. On account of current work, quality of water in the Baitarani basin, located in the State of Odisha, was recommended for its adaptability for human consumption and agriculture. A total of 13 sampling sites were chosen and its 22 parameters were investigated. The spatial intensity of several chemical and physical constituents throughout the research region was depicted using a GIS-based spatial analysis approach called IDW interpolation. Following the recommendations of the WHO, all physicochemical parameter's analytical findings were examined. It suggests:

- A minor increase in pH values indicates that the water is alkaline, probably as a result of fertilizer use in neighboring fields as well as other human sources. According to the following order, the primary cation and anion abundances are listed as $\text{Ca}^{2+} > \text{Na}^+ > \text{Mg}^{2+} > \text{K}^+$, which is equal to $\text{HCO}_3^- > \text{Cl}^- > \text{SO}_4^{2-} > \text{NO}_3^-$. Ca^{2+} along with HCO_3^- are the dominating cations and anions among the investigated ions.
- EWQI maps exhibit the category of water to showcase the medium good and susceptible areas for efficient water resource management. Based on EWQI classification shows excellent quality representing 15.385 of the samples, good quality representing 38.46% of the samples, medium quality representing 15.385 of the samples and poor quality representing 30.77% of the samples for drinking purposes. High value is mostly caused by high turbidity and total coliform levels. At St. 8, 11, 12, and 13, sewage, animal waste, settlement, usage of fertilizers, and runoff from urban areas all contributed to the poor water quality.
- MCDM based method like TOPSIS has been implemented in the concerned area and classified the water quality in St-8 as the most polluted location followed by St-12 and St-13 respectively.
- Further, irrigation water quality indexes including SAR, KI, RSC, PI, CAI-1, CAI-2, CR, PS and MH were calculated from the analysis and showed that the river water is suitable for irrigation throughout the monsoon period. However, PI needs to be managed because it can have dangerous consequences when used for irrigation.
- As per the Piper trilinear classification, the dominant water type is classified as $\text{Ca}(\text{HCO}_3)_2$. This is due to the water-rock interaction and anthropogenic contamination. According to Durov plots, the class of water is found to be as $\text{Na}^+ - \text{Cl}^-$ and mixed $\text{Ca}^{2+} - \text{Mg}^{2+} - \text{Cl}^-$ type. The bulk of the samples are in the

mixing phase, which is indicated by the predominance of dissolution with only a few in reverse ion exchange processes. Thus, alkalis dominate all hydrochemistry in nature mainly due to the presence of Na^+ .

- Most of surface water samples, according to the Wilcox model, exhibit low salinity hazard (S1) and low alkalinity hazard (C1). Gibb's diagram shows a growth in Na^+ and Cl^- ions and subsequent greater TDS as a result of contaminated water, caused by the effects of poor sanitation, nutrients for agriculture, and irrigation return. Almost all of the water samples in every site fall under the category of evaporation-precipitation type.

As a result of the work's limitations, we advise future research into the concentrations of other hazardous and heavy metals as well as the application of GIS and modelling methods for a more thorough understanding of the suitability of surface water for irrigation. It is intended that the knowledge gained from this research will assist decision-makers in taking the appropriate action to ensure sustainable agriculture in the study region. Future studies should concentrate on the causes of nutrient and organic matter pollution using statistical techniques. The outcomes of the mathematical model study were compared to those of self-organizing and soft computing concepts in the following section.

Acknowledgement

The author extends the appreciation to the State Pollution Control Board (SPCB), Odisha, for their generous assistance in supplying the required data and C.V. Raman Global University (CGU), Bhubaneswar, Odisha, for providing the necessary facilities for this innovative work.

References

- [1] Fentahun, A., Mechal, A., Karuppanan, S., 2023. Hydrochemistry and quality appraisal of groundwater in Birr River Catchment, Central Blue Nile River Basin, using multivariate techniques and water quality indices. *Environ. Monit. Assess.* 195, 655. <https://doi.org/10.1007/s10661-023-11198-6>.
- [2] Mir S, Bhat MS, Rather GM, Mattoo D (2021) Groundwater Potential Zonation using Integration of Remote Sensing and AHP/ ANP Approach in North Kashmir, Western Himalaya, India. *Remote Sens L* 5:41–58.
- [3] Muthusamy, B., Sithu, G.D.S., Ramamoorthy, A., Shankar, K., Gnanachandrasamy, G., Monica, C., Xiaozhong, H., 2022. Isotopic signatures, hydrochemical and multivariate statistical analysis of seawater intrusion in the coastal aquifers of Chennai and Tiruvallur District, Tamil Nadu, India. *Mar. Pollut. Bull.* <https://doi.org/10.1016/j.marpolbul.2021.113232>.
- [4] Kumar, M., Singh, P., Singh, P., 2022. Fuzzy AHP based GIS and remote sensing techniques for the groundwater potential zonation for Bundelkhand Craton Region, India. *Geocarto Int.* 37 (22), 6671–6694.
- [5] Balamurugan, P., Kumar, P.S., Shankar, K., Nagavinothini, R., Vijayasurya, K., 2020b. Non-carcinogenic risk assessment of groundwater in southern part of Salem District in Tamilnadu, India. *J. Chil. Chem. Soc.* 65 (1), 4697–4707. <https://doi.org/10.4067/S0717-97072020000104697>.
- [6] Das, A. (2023). Identification of Surface Water Contamination Zones and its Sources on Mahanadi River, Odisha Using Entropy-Based WQI and MCDM Techniques. *Engineering Research Transcripts*, 4, 67–92. https://doi.org/10.55084/grinrey/ERT/978-81-964105-1-3_5
- [7] Karunanidhi, D., Aravinthasamy, P., Deepali, M., Subramani, T., Shankar, K., 2021. Groundwater pollution and human health risks in an industrialized region of southern India: impacts of the COVID-19 lockdown and the monsoon seasonal cycles. *Arch. Environ. Contam. Toxicol.* 80, 259–276. <https://doi.org/10.1007/s00244-020-00797-w>.

- [8] Mohamed, N.A., Wachemo, A.C., Karuppanan, S., Duraisamy, K., 2022. Spatio-temporal variation of groundwater hydrochemistry and suitability for drinking and irrigation in Arba Minch Town, Ethiopia: An integrated approach using water quality index, multivariate statistics, and Gis. *Urban Clim.* 46, 101338 <https://doi.org/10.1016/j.uclim.2022.101338>
- [9] Melkamu, T., Bagyaraj, M., Adimaw, M., Ngusie, A., Karuppanan, S., 2022. Detecting and mapping flood inundation areas in Fogera-dera floodplain, Ethiopia during an extreme wet season using sentinel-1 data. *Phys. Chem. Earth, Parts A/B/C* 127, 103189. <https://doi.org/10.1016/j.pce.2022.103189>.
- [10] Haji, M., Karuppanan, S., Qin, D., Shube, H., Serre Kawo, N., 2021a. Potential human health risks due to groundwater fluoride contamination: A case study using multi- techniques approaches (GWQI, FPI, GIS, HHRA) in bilate river basin of Southern Main Ethiopian Rift, Ethiopia. *Arch Environ Contam Toxicol* 80, 277–293. <https://doi.org/10.1007/s00244-020-00802-2>.
- [11] Berhanu, K.G., Hatiye, S.D., 2020. Identification of Groundwater Potential Zones Using Proxy Data: Case study of Megech Watershed, Ethiopia. *J. Hydrol. Reg. Stud* 28, 100676.
- [12] Teshome, A., Halefom, A., Ahmad, I., Teshome, M., 2020. Fuzzy logic techniques and GIS-based delineation of groundwater potential zones: a case study of Anger River basin, Ethiopia. *Model. Earth Syst. Environ* 7, 2619–2628. <https://doi.org/10.1007/s40808-020-01035-x>.
- [13] Karuppanan, S., Panneerselvam, B., Haji, M., Murugesan, B., Shube, H., Serre Kawo, N., 2022. Evaluation of Groundwater Quality and Its Suitability for Drinking and Cultivation Practices in and around the Deltaic Regions of South India Using DWQI, IWQI, and GIS. *Climate Change Impact on Groundwater Resources*. Springer, Cham, pp. 181–200. https://doi.org/10.1007/978-3-031-04707-7_10.
- [14] Das, A. (2023). Water Criteria Evaluation for Drinking Purposes in Mahanadi River Basin, Odisha. In: Al Khaddar, R., Singh, S.K., Kaushika, N.D., Tomar, R.K., Jain, S.K. (eds) *Recent Developments in Energy and Environmental Engineering. TRACE 2022. Lecture Notes in Civil Engineering*, vol 333. Springer, Singapore. https://doi.org/10.1007/978-981-99-1388-6_20
- [15] Cho YC, Choi HM, Ryu IG, Kim SH, Shin DS, Yu SJ (2021) Assessment of water quality in the lower reaches Namhan river by using statistical analysis and water quality index (WQI). *J Korean Soc Water Environ* 37:114–127. <https://doi.org/10.15681/KSWE.2021.37.2.114>.
- [16] Hong, Z.; Zhao, Q.; Chang, J.; Peng, L.; Wang, S.; Hong, Y.; Liu, G.; Ding, S. Evaluation of Water Quality and Heavy Metals in Wetlands along the Yellow River in Henan Province. *Sustainability* 2020, 12, 1300. [CrossRef].
- [17] Sarkar, K.; Majumder, M. Application of AHP-Based Water Quality Index for Quality Monitoring of Peri-Urban Watershed. *Environ. Dev. Sustain.* 2021, 23, 1780–1798. [CrossRef].
- [18] Matta G, Kumar A, Nayak A, Kumar P, Kumar A, Tiwari AK (2020) Water quality and planktonic composition of river Henwal (India) using comprehensive pollution index and biotic-indices. *Trans Indian National Acad Eng.* <https://doi.org/10.1007/s41403-020-00094-x>.
- [19] Singh, A.K.; Sathya, M.; Verma, S.; Jayakumar, S. Spatiotemporal Variation of Water Quality Index in Kanwar Wetland, Begusarai, India. *Sustain. Water Resour. Manag.* 2020, 6, 1–8. [CrossRef].
- [20] Ranganathan, M., Karuppanan, S., Murugasen, B., Brhane, G.K., Panneerselvam, B., 2022. Assessment of Groundwater Prospective Zone in Adigrat Town and Its Surrounding Area Using Geospatial Technology. In: *Climate Change Impact on Groundwater Resources*. Springer, Cham, pp. 387–405. https://doi.org/10.1007/978-3-031-04707-7_21.
- [21] Teodorof L, Ene A, Burada A, Despina C, Seceleanu-Odor D, Trifanov C, Ibram O, Bratfanof E, Tudor MI, Tudor M, Cernisencu I (2021) Integrated assessment of surface water quality in Danube River Chilia Branch. *Appl Sci* 11(19):9172.

- [22] Zhang ZM, Zhang F, Du JL, Chen DC (2022) Surface water quality assessment and contamination source identification using multi-variate statistical techniques: a case study of the Nanxi River in the Taihu Watershed. *China Water* 14(5):778.
- [23] Das, A. (2023). Assessment of potability of surface water and its health implication in Mahanadi Basin, Odisha. *Materials Today: Proceedings*.
- [24] Genjula, W., Jothimani, M., Gunalan, J. Abebe, A. 2023. Applications of statistical and AHP models in groundwater potential mapping in the Mensa river catchment, Omo river valley, Ethiopia. *Model. Earth Syst. Environ.* <https://doi.org/10.1007/s40808-023-01765-8>.
- [25] Vijay, S., & Kamaraj, K. (2021). Prediction of Water Quality Index in Drinking Water Distribution System Using Activation Functions Based Ann. *Water Resources Management*, 35(2), 535–553. <https://doi.org/10.1007/s11269-020-02729-8>
- [26] Khan, M.Y.A., ElKashouty, M., Tian, F., 2022. Mapping groundwater potential zones using analytical hierarchical process and multicriteria evaluation in the Central Eastern Desert, Egypt. *Water* 14 (7), 1041. <https://doi.org/10.3390/w14071041>.
- [27] Wu, Z. & Abdul-Nour, G. 2020 Comparison of multi-criteria group decision-making methods for urban sewer network plan selection. *Civil Engineering* 1(1), 26–48.
- [28] Gupta, S. (2022). AHP-based multi-criteria decision-making for forest sustainability of lower Himalayan foothills in northern circle, India-a case study. *Environmental Monitoring and Assessment*, 194(12), 1– 11. <https://doi.org/10.1007/s10661-022-10510-0>.
- [29] Rashidi, F., & Sharifian, S. (2022). A comparative analysis of three multi-criteria decision-making methods for land suitability assessment. *Environmental Monitoring and Assessment*, 194(9), 1–15.
- [30] Behzadian, M., Otaghsara, S. K., Yazdani, M. & Ignatius, J. 2012 A state-of-the-art survey of TOPSIS applications. *Expert Systems with Applications* 39(17), 13051–13069.
- [31] Bera, A., Mukhopadhyay, B.P., Barua, S., 2020. Delineation of groundwater potential zones in Karha river basin, Maharashtra, India, using AHP and geospatial techniques. *Arab. J. Geosci* 13 (15). <https://doi.org/10.1007/s12517-020-05702-2>.
- [32] Soujanya Kamble B, Saxena PR, Kurakalva RM, Shankar K (2020) Evaluation of seasonal and temporal variations of groundwater quality around Jawaharnagar municipal solid waste dumpsite of Hyderabad City, India. *SN Appl Sci* 2:1–22. <https://doi.org/10.1007/s42452-020-2199-0>.
- [33] Agarwal M, Singh M, Hussain J (2020) Evaluation of groundwater quality for drinking purpose using different water quality indices in parts of Gautam Budh Nagar District, India. *ASIAN J Chem* 9:1128–1138.
- [34] Ijumulana, J., Ligate, F., Irunde, R., Bhattacharya, P., Maity, J. P., Ahmad, A. & Mtaló, F. 2021 Spatial uncertainties in fluoride levels and health risks in endemic fluorotic regions of northern Tanzania. *Groundwater Sustainable Dev.* 14, 100618
- [35] Anand B, Karunanidhi D, Subramani T, Srinivasamoorthy K, Suresh M (2020) Long-term trend detection and spatiotemporal analysis of groundwater levels using GIS techniques in Lower Bhavani River basin, Tamil Nadu, India. *Environ Dev Sustain* 22:2779–2800. <https://doi.org/10.1007/s10668-019-00318-3>.
- [36] Ifediegwu, S.I., 2021. Assessment of groundwater potential zones using GIS and AHP techniques: a case study of the Lafia district, Nasarawa State, Nigeria. *Appl. Water Sci*
- [37] Jothimani, M., Abebe, A., Berhanu, G. 2023. Applications of geospatial technologies and frequency ratio method in groundwater potential mapping in Iyenda River Catchment, Konso Area, Rift Valley, Ethiopia. In: Nandagiri, L., Narasimhan, M.C., Marathe, S. (eds) *Recent Advances in Civil Engineering. Lecture Notes in Civil Engineering*, vol 256. Springer, Singapore. https://doi.org/10.1007/978-981-19-1862-9_9

- [38] Sarfo AK, Shankar K (2020) Application of geospatial technologies in the COVID-19 fight of Ghana. *Transact Indian Nat Acad Eng* 5:193–204
- [39] Panneerselvam, B., Karuppannan, S., & Muniraj, K. (2020b). Evaluation of drinking and irrigation suitability of groundwater with special emphasizing the health risk posed by nitrate contamination using nitrate pollution index (NPI) and human health risk assessment (HHRA). *Human and Ecological Risk Assessment: An Int J*, pp 1–25.
- [40] Kumar, A., Kanga, S., Taloor, A. K., Singh, S. K. & Durin, B. 2021 Surface runoff estimation of Sind River basin using integrated SCS-CN and GIS techniques. *Hydro. Res.* 4,61–74. ISSN 2589-7578, <https://doi.org/10.1016/j.hydres.2021.08.001>.
- [41] Chabuk A, Al-Madhlom Q, Al-Maliki A, Al-Ansari N, Hussain HM, Laue J (2020) Water quality assessment along Tigris River (Iraq) using water quality index (WQI) and GIS software. *Arab J Geosci* 13(14):1–23. <https://doi.org/10.1007/s12517-020-05575-5>.
- [42] Das, A., Goya, A., & Soni, A. (2023, July). Use of water quality indices and its evaluation to verify the impact of Mahanadi River basin, Odisha. In *AIP Conference Proceedings* (Vol. 2721, No. 1). AIP Publishing.
- [43] Abdulkerim, E., Fufa, F., Takala, W., 2022. Identification of groundwater recharge site using geographical information system and remote sensing: case study of Sude district, Oromia, Ethiopia. *Environ. Earth Sci* 81 (2). <https://doi.org/10.1007/s12665-022-10170-w>.
- [44] Kumar D, Rajesh K, Mondal S, Warsi T, Rangarajan R (2020) Groundwater exploration in limestone–shale–quartzite terrain through 2D electrical resistivity tomography in Tadipatri, Anantapur district, Andhra Pradesh. *J Earth Syst Sci* 129(1):1–16. <https://doi.org/10.1007/s12040-020-1341-0>.
- [45] Das, A., Goyal, A., & Soni, A. (2023, July). Deciphering surface water quality for irrigation and domestic purposes: A case study in Baitarani Basin, Odisha. In *AIP Conference Proceedings* (Vol. 2721, No. 1). AIP Publishing.
- [46] Das, A. (2022). Multivariate statistical approach for the assessment of water quality of Mahanadi basin, Odisha. *Materials Today: Proceedings*.
- [47] Das, A. (2023). Assessment of Surface Water Quality by Means of MCDM Approach in Mahanadi River Basin (MRB), Odisha. *Resilience* 360, 51.
- [48] Laltu, A. D. (2023). Drinking Suitability and Source Apportionment of Physical Parameters in Surface Water in Mahanadi Basin, Odisha. *Odisha (April 14, 2023)*.
- [49] Jalees, M. I., Farooq, M. U. & Shah, A. T. 2021b Cancer risk assessment and modeling of groundwater contamination near industrial estate, Lahore, Pakistan. *Journal of Water, Sanitation and Hygiene for Development* 11(2), 314–326.
- [50] Das, A., & Tripathi, B. (2021). Water Quality and Hydrochemical Assessment for Irrigation on Baitarani River Basin, Odisha. *Journal of Mechanical and Civil Engineering*, 63-107.
- [51] Patra, T. R., Chakraborty, P., Naik, D., & Pathy, A. C. (2023). Environmental Change Analysis Using Remote Sensing and GIS: A Study of Upper Baitarani Basin, Odisha. In *Advanced Remote Sensing for Urban and Landscape Ecology* (pp. 283-297). Singapore: Springer Nature Singapore.
- [52] Atchyuth, B. A. S., Swain, R., & Das, P. (2023). Near Real-time Flood Inundation and Hazard Mapping of Baitarani River Basin using Google Earth Engine and SAR Imagery.
- [53] APHA. *Standard Methods for the Examination of Water and Wastewater*, 23rd ed.; American Public Health Association: Washington, DC, USA, 2017.
- [54] Dwivedi, P.P., Sharma, D.K., 2022. Application of Shannon Entropy and COCOSO techniques to analyze performance of sustainable development goals: The case of the Indian Union Territories. *Results in Engineering* 14, 100416.

- [55] Li P, Qian H, Wu J (2010) Groundwater quality assessment based on improved water quality index in Pengyang County, Ningxia, Northwest China. *J Chem* 7(S1):S209–S216.
- [56] Marghade D (2020) Detailed geochemical assessment & indexing of shallow groundwater resources in metropolitan city of Nagpur (western Maharashtra, India) with potential health risk assessment of nitrate enriched groundwater for sustainable development. *Geochemistry*. <https://doi.org/10.1016/j.chemer.2020.125627>.
- [57] Li, J., Wang, Y., Zhu, C., Xue, X., Qian, K., Xie, X., et al. (2020b). Hydrogeochemical Processes Controlling the Mobilization and Enrichment of Fluoride in Groundwater of the North China Plain. *Sci. Total Environ.* 730, 138877. <https://doi.org/10.1016/j.scitotenv.2020.138877>.
- [58] Wu J, Li P, Qian H (2011) Groundwater quality in Jingyuan County, a semi-humid area in Northwest China. *J Chem* 8(2):787–793.
- [59] Hwang, C. L. & Yoon, K. 1981 Multiple Attribute Decision Making Methods and Applications. Springer, Berlin, Heidelberg, p. 259.
- [60] Varatharajulu, M., Duraiselvam, M., Kumar, M. B., Jayaprakash, G., & Baskar, N. (2022). Multi criteria decision making through TOPSIS and COPRAS on drilling parameters of magnesium AZ91. *Journal of Magnesium and Alloys*, 10, 2857–2874.
- [61] Huang, W., Shuai, B., Sun, Y., Wang, Y. & Antwi, E. 2018 Using ENTROPY-TOPSIS method to evaluate urban rail transit system operation performance: the China case. *Transportation Research Part A: Policy and Practice* 111, 292–303.
- [62] Hamid, A., Bhat, S.U., Jehangir, A., 2020. Local determinants influencing stream water quality. *Appl. Water Sci.* 10 (24), 1–16.
- [63] Kumar A, Krishna AP (2021) Groundwater quality assessment using geospatial technique-based water quality index (WQI) approach in a coal mining region of India. *Arab J Geosci* 14. <https://doi.org/10.1007/s12517-021-07474-9>.
- [64] Angello, Z.A., Tränckner, J., Behailu, B.M., 2020. Spatio-temporal evaluation and quantification of pollutant source contribution in little Akaki river, Ethiopia: conjunctive application of factor analysis and multivariate receptor model. *Pol. J. Environ. Stud.* 30 (1), 23–34. <https://doi.org/10.15244/pjoes/119098>.
- [65] WHO (2017) Guideline for drinking water quality, 4th edn. World Health Organization, Geneva
- [66] Aravinthasamy, P., Karunanidhi, D., Shankar, K., Subramani, T., Setia, R., Bhattacharya, P., Das, S., 2021. COVID-19 lockdown impacts on heavy metals and microbes in shallow groundwater and expected health risks in an industrial city of South India. *Environ. Nanotechnol. Monitor. Manag.* 16, 100472 <https://doi.org/10.1016/j.enmm.2021.100472>.
- [67] Aydin, H., Ustaoglu, F., Tepe, Y., Soyulu, E.N., 2020. Assessment of water quality of streams in northeast Turkey by water quality index and multiple statistical methods. *Environ. Forensics* 22 (1–2), 270–287.
- [68] Kadam, A., Wagh, V., Jacobs, J., Patil, S., Pawar, N., Umrikar, B., Sankhua, R., Kumar, S., 2021. Integrated approach for the evaluation of groundwater quality through hydro geochemistry and human health risk from Shivganga river basin. *Environ. Sci. Pollut. Res., Pune, Maharashtra, India* 29 (3), 4311–4333. PMID: 34403054.
- [69] Ustaoglu, F., Tepe, Y., and Tas, B. 2020. Assessment of stream quality and health risk in a subtropical Turkey river system: A combined approach using statistical analysis and water quality index. *Ecological Indicators* 113(105815):1-12.
- [70] Tore, Y., Ustaoglu, F., Tepe, Y., Kalipci, E., 2021. Levels of toxic metals in edible fish species of the Tigris River (Turkey); threat to public health. *Ecol. Indicat.* 123, 107361.

- [71] Aliyu, A.G., Jamil, N.R.B., Adam, MB bin, Zulkeflee, Z., 2020. Spatial and seasonal changes in monitoring water quality of Savanna River system. *Arabian J. Geosci.* 13 (2), 1–13.
- [72] Ameen, H.A., 2019. Spring water quality assessment using water quality index in villages of Barwari Bala, Duhok, Kurdistan Region, Iraq. *Appl. Water Sci.* 9 (8), 1–12.
- [73] Allafta, H., Opp, C. & Patra, S. 2021 Identification of groundwater potential zones using remote sensing and GIS techniques: a case study of the Shatt al-Arab Basin. *Remote Sens.* 13,1–28. <https://doi.org/10.3390/rs13010112>
- [74] Arunbose, S., Srinivas, Y., Rajkumar, S., Nair, N. C. & Kaliraj, S. 2021 Remote sensing, GIS and AHP techniques based investigation of groundwater potential zones in the Karumeniyar river basin, Tamil Nadu, southern India. *Groundwater Sustainable Dev.* 14, 100586. <https://doi.org/10.1016/J.GSD.2021.100586>.
- [75] Tadesse, M., Tsegaye, D., and Girma, G. (2018). Assessment of the level of some physico-chemical parameters and heavy metals of Rebu river in oromia region. *Ethiopia.* 2, 885. doi: 10.15406/mojbm.2018.03.00085.
- [76] Gad, M.; Elsayed, S.; Moghanm, F.S.; Almarshadi, M.H.; Alshammari, A.S.; Khedher, K.M.; Eid, E.M.; Hussein, H. Combining Water Quality Indices and Multivariate Modeling to Assess Surface Water Quality in the Northern Nile Delta, Egypt. *Water* 2020, 12, 2142. [CrossRef].
- [77] Ezugwu, C.K., Onwuka, O.S., Egbueri, J.C., Unigwe, C.O., Ayejoto, D.A., 2019. Multi- criteria approach to water quality and health risk assessments in a rural agricultural province, southeast Nigeria. *HydroResearch* 2, 40–48.
- [78] Richards LA (U.S. Salinity Laboratory) (1954) Diagnosis and improvement of saline and alkaline soils, U.S. Department of Agriculture Hand Book.
- [79] Wilcox LV (1995) Classification and use of irrigation waters. US Department of Agriculture, Washington DC.
- [80] Saha, S., Reza, A.H.M.S., Roy, M.K., 2019. Hydrochemical evaluation of groundwater quality of the Tista floodplain, Rangpur, Bangladesh. *Appl. Water Sci.* 9 (8), 1–12.
- [81] Paliwal K V 1972 Irrigation with saline water; Monogram no. 2 (New series), New Delhi, IARI, 198p.
- [82] Kelly W P 1963 Use of saline irrigation water; *Soil Science* 95(4) 355–391.
- [83] Berhe, B.A., 2020. Evaluation of groundwater and surface water quality suitability for drinking and agricultural purposes in Kombolcha town area, eastern Amhara region, Ethiopia. *Appl. Water Sci.* 10 (6), 1–17.
- [84] Rawat KS, Singh SK, Gautam SK (2018) Assessment of groundwater quality for irrigation use: a peninsular case study. *Appl Water Sci* 8:233. <https://doi.org/10.1007/s13201-018-0866-8>.
- [85] Sharma RC, Tiwari V (2018) Seasonal physico-chemical characterization of water of sacred lake Nachiketa Tal, Garhwal Himalaya. *Appl Water Sci* 8:1–9. <https://doi.org/10.1007/s13201-018-0802-y>.
- [86] Egbueri, J.C., 2022. Predicting and analysing the quality of water resources for industrial purposes using integrated data-intelligent algorithms. *Groundwater Sustain. Dev.* 100794.
- [87] Doneen LD (1964) Notes on water quality in Agriculture Published as a Water Science and Engineering Paper 4001, Department of Water Science and Engineering, University of California.
- [88] Revelle R (1941) Criteria for recognition of sea water in ground- waters. *Trans Amer Geophys Union* 22:593–597.
- [89] Sunkari, E.D., Abu, M., Zango, M.S., Lomoro, Wani, A.M., 2020. Hydrogeochemical characterization and assessment of groundwater quality in the Kwahu-Bombouaka Group of the Voltaian Supergroup, Ghana. *J. Afr. Earth Sci.* 169 (November 2019), 103899 <https://doi.org/10.1016/j.jafrearsci.2020.103899>.

- [90] Durov S (1948) Classification of natural waters and graphic presentation of their composition. Dokl Akad Nauk SSSR 1:87–90.
- [91] Piper AM (1944) A graphic procedure in the geochemical interpretation of water-analyses. Eos, Trans Am Geophys Union 25:914–928. <https://doi.org/1029/TR025i006p00914>.
- [92] Zhou, M., Li, X., Zhang, M., Liu, B., Zhang, Y., Gao, Y., et al., 2020. Water quality in a worldwide coal mining city: a scenario in water chemistry and health risks exploration. *J. Geochem. Explor.* 213, 106513.
- [93] Gibbs, R. J. 1970 Mechanisms controlling world water chemistry. *Science, New Series* 170(3962), 1088–1090. <http://www.jstor.org/stable/1730827>
- [94] Liu, J., Peng, Y., Li, C., Gao, Z., Chen, S., 2021. An investigation into the hydrochemistry, quality and risk to human health of groundwater in the central region of Shandong Province, North China. *J. Clean. Prod.* 282, 125416.
- [95] Mekonnen, B., Haddis, A., Zeine, W., 2020. Assessment of the effect of solid waste dump site on surrounding soil and River Water quality in tepi town, southwest Ethiopia. *J. Environ. Public Health* 2020, 1–9.
- [96] Kumar, S., Islam, A. R. M. T., Hasanuzzaman, M., Salam, R., Khan, R., and Islam, M. S. (2021). Preliminary assessment of heavy metals in surface water and sediment in Nakuvadra-Rakiraki River, Fiji using indexical and chemometric approaches. *J. Environ. Manage.* 298, 113517. doi: 10.1016/j.jenvman.2021.113517.
- [97] Subba Rao N (2017) *Hydrogeology: problems with solutions*. Prentice Hall of India, New Delhi.
- [98] Gugulothu, S., Subbarao, N., Das, R. & Dhakate, R. 2022 Geochemical evaluation of groundwater and suitability of groundwater quality for irrigation purpose in an agricultural region of South India. *Applied Water Science* 12(6), 1–13. <https://doi.org/10.1007/s13201-022-01583-w>
- [99] Kammoun, A., Abidi, M. & Zairi, M. 2022 Hydrochemical characteristics and groundwater quality assessment for irrigation and drinking purposes: a case of Enfidha aquifer system, Tunisia. *Environmental Earth Sciences* 81(2), 1–15. <https://doi.org/10.1007/s12665-021-10163-1>.